NASA/TM–20210013649

Segregation Evolution and Diffusion of Titanium in Directed Energy Deposited NASA HR-1

P.S. Chen,[1] C.C. Katsarelis,[2] W.M. Medders,[1] and P.R. Gradl[2]

[1]Jacobs ESSCA Group, Huntsville, Alabama
[2]Marshall Space Flight Center, Huntsville, Alabama

May 2021

The NASA STI Program…in Profile

Since its founding, NASA has been dedicated to the advancement of aeronautics and space science. The NASA Scientific and Technical Information (STI) Program Office plays a key part in helping NASA maintain this important role.

The NASA STI Program Office is operated by Langley Research Center, the lead center for NASA's scientific and technical information. The NASA STI Program Office provides access to the NASA STI Database, the largest collection of aeronautical and space science STI in the world. The Program Office is also NASA's institutional mechanism for disseminating the results of its research and development activities. These results are published by NASA in the NASA STI Report Series, which includes the following report types:

- TECHNICAL PUBLICATION. Reports of completed research or a major significant phase of research that present the results of NASA programs and include extensive data or theoretical analysis. Includes compilations of significant scientific and technical data and information deemed to be of continuing reference value. NASA's counterpart of peer-reviewed formal professional papers but has less stringent limitations on manuscript length and extent of graphic presentations.

- TECHNICAL MEMORANDUM. Scientific and technical findings that are preliminary or of specialized interest, e.g., quick release reports, working papers, and bibliographies that contain minimal annotation. Does not contain extensive analysis.

- CONTRACTOR REPORT. Scientific and technical findings by NASA-sponsored contractors and grantees.

- CONFERENCE PUBLICATION. Collected papers from scientific and technical conferences, symposia, seminars, or other meetings sponsored or cosponsored by NASA.

- SPECIAL PUBLICATION. Scientific, technical, or historical information from NASA programs, projects, and mission, often concerned with subjects having substantial public interest.

- TECHNICAL TRANSLATION. English-language translations of foreign scientific and technical material pertinent to NASA's mission.

Specialized services that complement the STI Program Office's diverse offerings include creating custom thesauri, building customized databases, organizing and publishing research results…even providing videos.

For more information about the NASA STI Program Office, see the following:

- Access the NASA STI program home page at <http://www.sti.nasa.gov>

- E-mail your question via the Internet to <help@sti.nasa.gov>

- Phone the NASA STI Help Desk at 757–864–9658

- Write to:
  NASA STI Information Desk
  Mail Stop 148
  NASA Langley Research Center
  Hampton, VA 23681–2199, USA

NASA/TM–20210013649

Segregation Evolution and Diffusion of Titanium in Directed Energy Deposited NASA HR-1

P.S. Chen,[1] C.C. Katsarelis,[2] W.M. Medders,[1] and P.R. Gradl[2]

[1]Jacobs ESSCA Group, Huntsville, Alabama
[2]Marshall Space Flight Center, Huntsville, Alabama

National Aeronautics and
Space Administration

Marshall Space Flight Center • Huntsville, Alabama 35812

May 2021

Acknowledgements

Additive manufacturing and new materials are advancing and multiple people and organizations are responsible for the development and advancement of NASA HR-1. The authors would like to thank the SLS Liquid Engines Office (LEO) program and Rapid Analysis and Manufacturing Propulsion Technology (RAMPT) project for providing funding and support to develop the processes and advancing this alloy. We would like to thank Steve Wofford, Johnny Heflin, John Fikes, Jessica Wood, and Robert Hickman who provided project leadership. We would like to acknowledge our industry and academia partners including RPM Innovations (RPMI), BeAM, Fraunhofer, Formalloy, Nima Shamsaei, and Mike Ogles at Auburn University (RAMPT Public Private Partner), and Judy Schneider at University of Alabama Huntsville (UAH) for partnering to develop the process, development, and characterizing samples. We would also like to acknowledge various vendors providing feedstock powder including Homogenized Metals, Inc., (HMI), Praxair, and Powder Alloy Corporation (PAC). Heat treating is a critical operation, and our experts Pat Salvail, Kenny Webster, and David Cole provided outstanding support. We would also like to thank the NASA Glenn Research Center (GRC) counterparts including Laura Evans, David Ellis, Justin Milner, Chris Kantzos, Ivan Locci, and many others who have helped evaluate and characterize samples. Additionally, we recognize the other engineers who have provided inputs throughout development including Chris Protz, Will Tilson, Brian West, Catherine Bell, Samantha McLeroy, and the many others at NASA Marshall Space Flight Center and GRC.

Available from:

NASA STI Information Desk
Mail Stop 148
NASA Langley Research Center
Hampton, VA 23681–2199, USA
757–864–9658

This report is also available in electronic form at
<http://www.sti.nasa.gov>

TABLE OF CONTENTS

LIST OF FIGURES

LIST OF FIGURES (Continued)

LIST OF TABLES

LIST OF ACRONYMS, ABBREVATIONS

AB	as-built
Al	aluminum
AM	additive manufacturing
Ar	argon
CAD	computer-aided design
CNC	computer numerical control
Co	cobalt
Cr	chromium
DED	directed energy deposition
EDS	energy-dispersive x-ray spectroscopy
FCC	face centered cubic
Fe	iron
GCP	geometrically-closed-pack intermetallic phases (e.g., η, δ phases)
HAZ	heat affected zone
HEE	hydrogen environment embrittlement
HIP	hot isostatic press
ICP	inductively coupled plasma (mass spectrometry)
LCF	low cycle fatigue
LEO	liquid engines office
LP DED	laser powder directed energy deposition

LIST OF ACRONYMS, ABBREVATIONS (Continued)

LRE	liquid rocket engine
Mo	molybdenum
MSFC	Marshall Space Flight Center
Ni	nickel
Ni_3Ti	nickel compound, with titanium (3:1)
PHACOMP	phase computation
RAMPT	Rapid Analysis and Manufacturing Propulsion Technology
Rev	revision
SA	solution anneal
SEM	scanning electron microscopy
SLS	Space Launch System
SR	stress relief
TCP	topologically-close d-pack intermetallic phases (e.g., σ, χ, laves phases)
Ti	titanium
TRL	technology readiness level
V	vanadium
VAR	vacuum arc remelt
VIM	vacuum induction melting
W	tungsten
γ	ni-fe matrix phase
γ'	precipitate phase ($Ni_3(Ti,Al)$)
η-phase	nickel titanium (Ni_3Ti)

NOMENCLATURE

$C_{0_{max}}$	grain boundary solute atom concentration before homogenization
$C_{0_{min}}$	grain center solute atom concentration before homogenization
C_A	initial amplitude of titanium segregation
C_m	mean titanium concentration (after complete homogenization)
C_{max}	grain boundary solute atom concentration after homogenization
C_{min}	grain center solute atom concentration after homogenization
D	diffusivity (diffusion coefficient)
D_o	diffusion constant (m^2/s)
D_X	discrete variational (DX)-Xα cluster method
HOM	homogenization
L	half wavelength of titanium concentration
Md	d-orbital energy level
Q	diffusion activation energy (J/mole)
R	gas constant (8.31 J/mole-K)
T	thermodynamic temperature
δ	residual segregation index

TECHNICAL MEMORANDUM

SEGREGATION EVOLUTION AND DIFFUSION OF TITANIUM IN DIRECTED ENERGY DEPOSITED NASA HR-1

1. INTRODUCTION

NASA HR-1 is a high-strength iron-nickel (Fe-Ni) superalloy designed to resist high pressure, hydrogen environment embrittlement, oxidation, and corrosion. NASA HR-1 was originally developed at NASA in the 1990s and derived from JBK-75 to increase strength and ductility in high-pressure hydrogen environments. The NASA HR-1 chemistry was formulated to meet requirements for liquid rocket engine (LRE) applications, specifically components used in a high-pressure hydrogen environment. LRE components provide extreme and challenging environments for materials throughout engine operation. Component structures used in LREs can require very thin walls—in regeneratively-cooled nozzles, for instance—that provide challenges with thermal and structural loads. Additionally, combining the environment with liquid and gaseous hydrogen propellant with the thermal and structural loads provide an even more complex challenge. For these applications, materials must be designed to resist hydrogen environment embrittlement (HEE). Furthermore, these components have key requirements to consider for materials selection, including thermal conductivity, low cycle fatigue (LCF), yield strength, and elongation.

While a few materials are available to meet these requirements, there are trades that must be made amongst the various properties during operation, which could make the design heavier than necessary or lead to premature failure due to low margins. Aerospace structural alloys that encounter gaseous hydrogen in operation (for example, hot gas manifolds in a rocket engine and hotwall of a rocket nozzle) require adequate resistance to HEE in addition to good strength and oxidation/corrosion resistance. Austenitic stainless steels (such as 304, 310, and 316) are hydrogen resistant but have low yield strength (around 276 MPa). Iron-base superalloys that are derived from austenitic stainless steels (such as A-286, and JBK-75) have adequate resistance to HEE, corrosion, and oxidation but lack high strength. In consideration of these problems, NASA HR-1 was specifically developed[1] as a higher strength structural alloy that has combined virtues of HEE, oxidation, and corrosion resistance.

When NASA HR-1 was being designed, it was evident that hydrogen-resistant iron-base superalloys, such as A-286, JBK-75,[2] have γ-matrix compositions evolving from hydrogen-resistant stainless steels (single γ-phase materials). The alloy development was approached by formulating a hydrogen-resistant γ-matrix that resembles JBK-75 along with increasing γ' volume fraction and strengthening γ-matrix. The matrix phase, γ, is a solid solution of iron, nickel, cobalt (Co), chromium (Cr), molybdenum (Mo), tungsten (W), and vanadium (V); whereas the precipitate phase γ' is composed of hardening elements titanium (Ti) and aluminum (Al). Another precipitate phase

was observed in the microstructure, nickel titanium (3:1), also known as (Ni_3Ti) or η-phase. This η-phase is a titanium-rich acicular precipitate that forms along grain boundaries under certain heat-treated conditions, and it forms within the grains after prolonged exposure to elevated temperatures. Using the hydrogen-resistant γ-matrix as a foundation, the rationale for the alloy chemistry for NASA HR-1 follows the subsequent criteria:

- The iron:nickel ratio was varied to improve solid solubility and to identify HEE-resistant compositional ranges. Higher nickel can reduce solidification and HAZ cracking susceptibility.[1,3]

- Volume fraction of γ' was increased by adding more titanium and aluminum for higher strength without super-saturating of the γ-matrix by requiring more nickel and/or cobalt to avoid detrimental η-phase.[4,5]

- Cobalt was added to reduce *Md* value so that the iron:nickel ratio can be kept close to that of JBK-75.

- Tungsten was added to strengthen the γ-matrix and to retard η precipitation in the grain boundaries.[6,7]

- Molybdenum content was increased to 2.0% to strengthen the γ-matrix and to reduce solidification and HAZ cracking susceptibility.[1,3]

- Chromium content was kept at 14.0%–16.0% to preserve corrosion/oxidation resistance. Tungsten was kept at the same level as JBK-75 to improve resistance to notch effect and hot formability.

Phase computation (PHACOMP) analysis was used for NASA HR-1 development to evaluate the phase stability of the experimental alloy.[8] This concept was devised based on molecular orbital calculation (the discrete variational (*DX*)-*Xα* cluster method) for transition-metal-based alloys. The primary parameter used is the *d*-orbital energy level (*Md*) of alloying transition metal elements. The *d*-orbital energy above the Fermi energy level for the transition metals, denoted by *Md*, has been used to estimate the solubility limit of the terminal solid solution in transition-metal-based alloys.[8–10] The PHACOMP-value *Md* for NASA HR-1 was kept close to that of JBK-75 to maintain γ-matrix stability and minimize η precipitation.

NASA HR-1 is potentially an enabling material for use in high-pressure, high-temperature, hydrogen-based LRE components. However, the existing vacuum induction melting/vacuum arc remelting (VIM/VAR) processes and supply chain would not support cost trades, and alternate fabrication methods would have to be explored. Additive manufacturing technologies provided a critical method for affordable fabrication of NASA HR-1 and a simplified powder and fabrication supply chain. NASA started exploring alternate AM technology as part of the Marshall Space Flight Center (MSFC) Liquid Engines Office (LEO) Technology Development for RS-25 product improvement and under the Rapid Analysis and Manufacturing Propulsion Technology (RAMPT)

project using the NASA HR-1 material for channel wall nozzles and potentially other LRE components. For many of these applications, laser powder directed energy deposition (LP-DED) is being explored to build these components due to the scale of the components being developed.

Additive manufacturing (AM) technologies have enabled NASA HR-1 to become a cost-effective alloy by simplifying the material and fabrication supply chain. The LP-DED process can form near-net shape blanks, final-shape components, and integral channels and features within components. This special DED process provides the ability to significantly reduce part count and eliminate many of the process steps typically required for forming the liner, channel slotting, and closing out the coolant channels for nozzles.[11] This alternative DED technology is very attractive for these reasons but at a lower technology readiness level (TRL). NASA's goal was to evaluate the LP-DED technology and mature the process for integral channel wall nozzles, material characterization and properties, and complete hot fire testing in relevant environments.

The LP-DED process is being studied for several applications of regeneratively-cooled nozzles. This includes forming near-final shape components such as liners, manifolds, and an integrated-channel configuration to minimize part count. A significant advantage of the DED processes is the ability to adapt to a robotic or Gantry CNC system with a localized purge or purge chamber, allowing unlimited build volume. Much of the current focus of the DED is being explored to form the entire channel wall nozzle with integral coolant channels within a single AM build. This relies on the DED-fabrication of complex and thin-walled features. Characterization of the material properties produced with this technique is required in order to evolve this process.[12]

The LP-DED fabrication technique uses a coaxial nozzle with a central laser source and powder injected (or blown) into the laser focus. The melt pool is created by the coaxial laser energy source causing a weld bead to be deposited. The powder is accelerated, or blown, into the melt pool using an inert carrier gas to allow for minimal or reduced oxidation in the high temperature deposited/weld. This head system, with integrated focus optics and blown powder nozzle(s), is attached to a robot or gantry system that controls a toolpath defined by the CAD model. The blown powder head can be contained in an inert gas chamber or operated with a local purge. The blown powder system and robot allows complex freeform structures to be built with small integral features, such as thin-walls and channels. Various optics can be used to vary the laser spot size and consequently the melt pool width, which control the size of features that can be built. A picture of the process can be seen in Figure 1. Prior publications have delved into the design details of the DED process for nozzles and other components.[12–15]

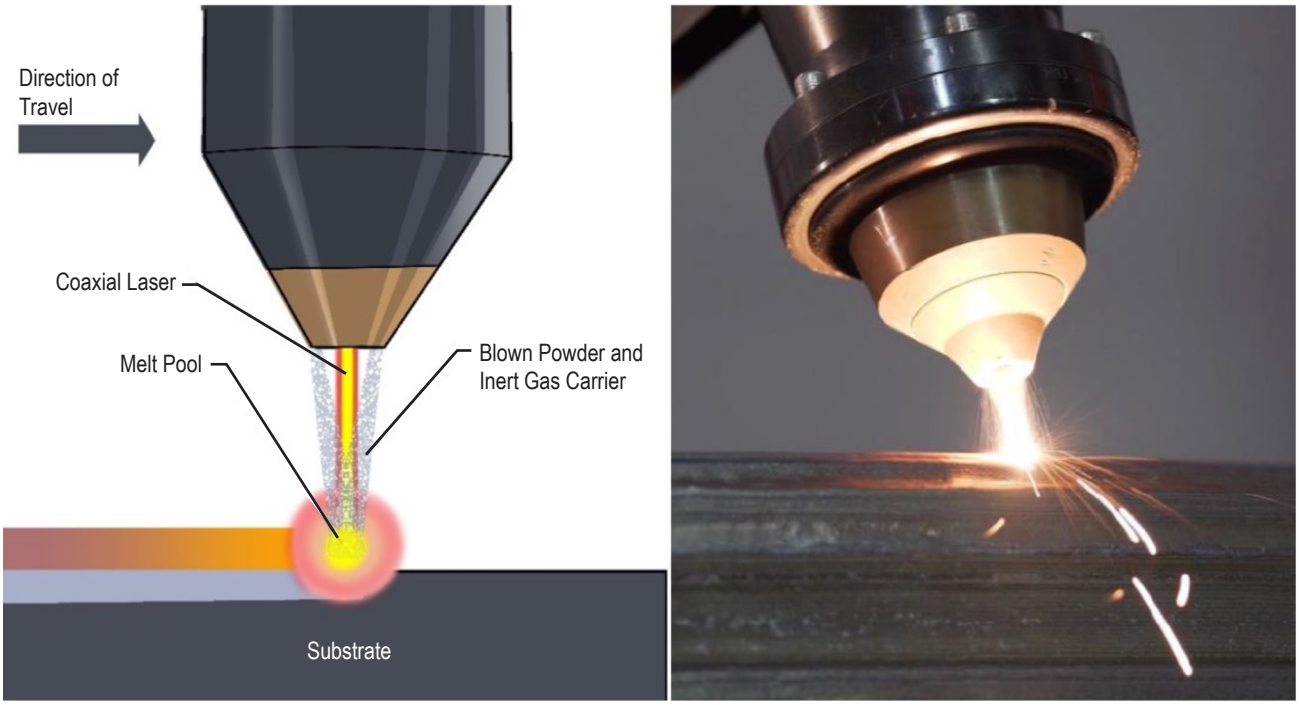

Figure 1. Overview of LP-DED Process.

The DED processed materials require several post-processing heat treatment steps in order to attain the materials properties that are desirable for the application. These steps often include a stress relief (SR), homogenization (HOM) or hot isostatic press (HIP), solution anneal (SA), and aging treatment for precipitation hardened alloys.[16] An effective stress relief mitigates residual stresses built up in the part during the DED process and minimizes the potential distortions before further post-processing. The second step, homogenization or HIP, is a common treatment for AM materials to reduce elemental segregation and promote recrystallization to achieve a more uniform equiaxed grain structure in the material. The third step, solution anneal, brings the part to a solid solution temperature to dissolve undesirable η-phase, which forms during cooling from homogenization treatment and then rapidly cooled to below 1200 F° to maintain η-phase free solid solution. Finally, the aging treatment promotes the precipitation of the strengthening phase in the alloy, the γ' phase for NASA HR-1.[1]

The as-deposited DED NASA HR-1 (revision 2 composition) has a high degree of titanium segregation in the interdendritic regions. Titanium segregation promotes precipitation of η-phase (Ni_3Ti) at grain boundaries that is detrimental to tensile ductility, LCF life, and resistance to hydrogen environment embrittlement. In order to achieve the optimum properties, as-built DED structures must be homogenized to reduce elemental segregations. The grain size is driven by the heating and solidification rates of the material during the deposit process, which is affected by several factors in LP-DED including part geometry, pass overlap, spot size, power, travel speed, powder feed rate, etc.[17] Due to the presence of high internal stresses in the DED materials, homogenization is accompanied by recrystallization and grain growth. Therefore, titanium segregation migrates from the interdendritic regions (in as-built DED material) to grain boundaries

after homogenization treatment. Thus, for DED NASA HR-1, the degree of homogenization is connected with the size of grains instead of the dendrite arm spacing in the as-built structure. Segregation of titanium in single-pass DED NASA HR-1 is extremely difficult to control because grain size varies considerably from zone to zone, and many large grains (>100 μm) are present after homogenization treatment. Therefore, it is of great importance to understand the segregation evolution and diffusion behavior of titanium so that appropriate heat treatment can be developed to mitigate titanium segregation.

In this Technical Memorandum, titanium segregation evolution during DED process and after high-temperature homogenization in DED NASA HR-1 was investigated. Homogenization kinetic analysis was performed to see how the homogenization treatment parameters should be adjusted to minimize the negative effects of severe titanium segregation. An analytical evaluation of homogenization for DED NASA HR-1 with different grain sizes was performed. A basic model for titanium diffusion in NASA HR-1 has been developed, which can project concentration distribution of titanium between grain boundaries as a function of homogenization temperature, duration, and grain size. The results of the homogenization kinetic analysis provide a valuable reference on how the homogenization treatment should be adjusted for DED NASA HR-1 (with large-grained structure) to reduce titanium segregation to a very low level.

2. EXPERIMENTAL PROCEDURES AND METHODS

2.1 Material and Directed Energy Depositing Process

The material used for the present study was as-built single-pass DED NASA HR-1 panels furnished by RPM Innovations (RPMI). The single-pass DED panels were deposited with a thickness of approximately 3.175 mm (1070 W) for thick panels and 1 mm (350 Watts laser) for the thin panels. The DED process was conducted with a single pass per layer that are parallel to the previous layer. The feedstock NASA HR-1 powder used for the DED process was a pre-alloyed, gas-atomized powder supplied by Praxair (FE-419-C62 Lot 1) using vacuum or inert induction melting gas atomization in argon (Ar). NASA HR-1 powder is primarily spherical in shape, free of significant satellite particles, and has a smooth surface. The powder size distribution is between 44 and 105 μm (–140 mesh/+325 mesh). The nominal and measured (by ICP) chemical composition (wt%) of NASA HR-1 powder is given in Table 1. The single-pass DED panel used in this study is shown in Figure 2.

Table 1. Nominal and measured chemical composition (wt%) of NASA HR-1 powder.

Alloy	Fe	Ni	Cr	Mo	V	W	Co	Ti	Al
NASA HR-1 powder (nominal, Rev 2)	39.80	34.00	15.50	2.20	0.32	2.10	3.30	2.50	0.25
NASA HR-1 powder (measured, Rev 2)	40.47	34.19	14.59	2.30	0.35	1.78	3.48	2.53	0.31

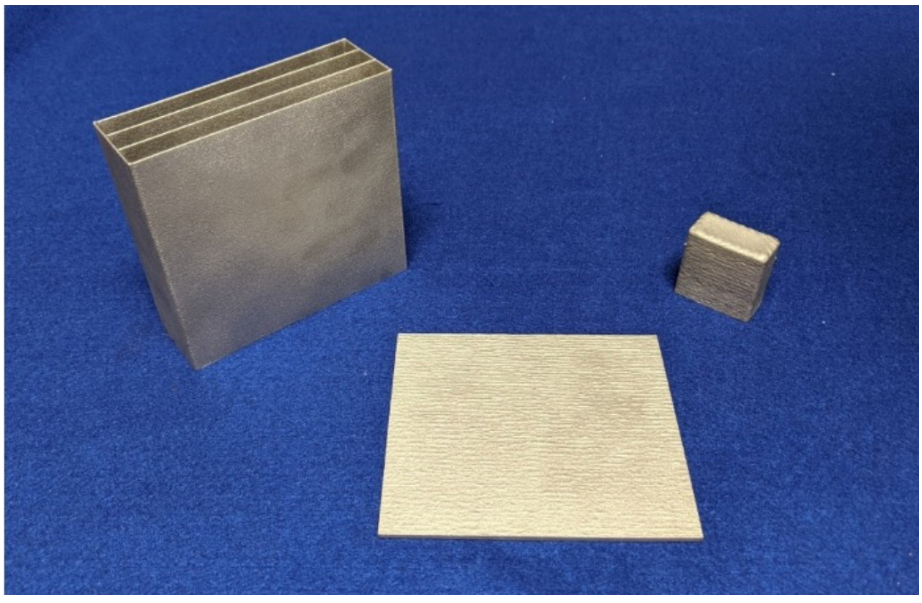

Figure 2. The single-pass LP-DED NASA HR-1 witness panel (left) used for materials characterization in this study.

2.2 Heat Treatment

After the deposition process, parts require several post-processing heat treatment steps to attain the materials properties that are desirable for the application. For DED NASA HR-1 parts, these steps include a stress relief, homogenization or HIP, solution anneal, and aging treatment. The initial as-built samples received stress-relief treatment at 1800 °F/1.5hr. After stress relief, the samples were initially subjected to a homogenization treatment at 2125 °F/3hr in a vacuum furnace. At the end of homogenization treatment, the samples were argon quenched to minimize η-phase precipitation. Then the samples were solution annealed at 1800 °F/1hr (followed by direct water quenching) and then aged at 1325 °F/16hr to complete the heat treatment process.

2.3 Metallography

Samples of DED NASA HR-1 were metallurgically characterized after every stage of heat treatment. Specimens were sectioned, mounted, ground, and polished using standard metallographic procedures with a series of 220–2,000 grit paper and 3-μm diamond suspension to 0.05-μm alumina pads. Chemical etching was conducted with waterless Kalling's reagent immersed for 5–10 s. Microstructures of as-deposited and heat-treated NASA HR-1 were examined via optical (Leica DMi8 A) and scanning electron microscopy (SEM) (Hitachi S-3700N) equipped with an energy-dispersive X-ray spectroscopy (EDS) detector (Oxford Instruments X-maxN 80). High-resolution optical montage images were taken to document the microstructure for the entire sample. Elemental analysis was conducted using EDS line scans across the edge of the specimen at 15 kV and 0.5 μm between spectra.

2.4 Analysis of Titanium Segregation

Investigation of titanium segregation was carried out using an EDS detector attached to an SEM. For as-deposited samples, EDS line scans were performed across the solidification structure, which has a minimum distance of 250 μm to reveal the concentration profile of titanium. For heat-treated samples, the EDS line scans must be greater than 250 μm and across at least one grain (two grain boundaries) to see the fluctuation of titanium concentration between grain boundaries and grain interior. In order to analyze the homogenization process in theory, homogenization kinetic calculations were performed to determine the titanium concentration distribution between grain boundaries as a function of homogenization temperature, time, and grain size.

3. RESULTS AND DISCUSSIONS

3.1 As-Built Microstructure

A representative vertical cross section macrostructure of an as-built DED panel is shown in Figure 3. This panel, approximately 3.175 mm thick, was deposited with single passes (1070 W) per layer that are parallel to the previous layer. The melt pool boundary is readily apparent in the as-built material. The columnar dendrites, which are common in high-energy AM processes, are shown in greater detail in Figure 3(b). In the high-energy process and rapid cooling system, the growing grains (and dendrites) align themselves with the sharp temperature gradients and result in columnar structure morphology.[18] The dendrites exhibit a pattern of formation from the outer perimeter of the melt pool toward a central point in single-pass DED NASA HR-1. The large temperature gradient provides suitable conditions for epitaxial dendrite (grain) growth as evidenced by the dendrites in the new layers are formed with the same orientation as the previous layers through several melt pools. The dendrites are somewhat randomly oriented near the melt pool periphery (toward the panel outer surface) likely due to the complex temperature gradient from the melt pool to the surrounding material. Closeup view of the dendritic structure in the as-built single-pass DED NASA HR-1 is shown in Figure 4. The size of dendrite cell is very small, and the primary dendrite arm spacing is in most cases smaller than 25 μm. Solute rejection of alloying elements to the interdendritic regions on solidification leads to the preferential attack upon etching. As a result, the existence of titanium segregation is revealed as the dark spots in the interdendritic regions.

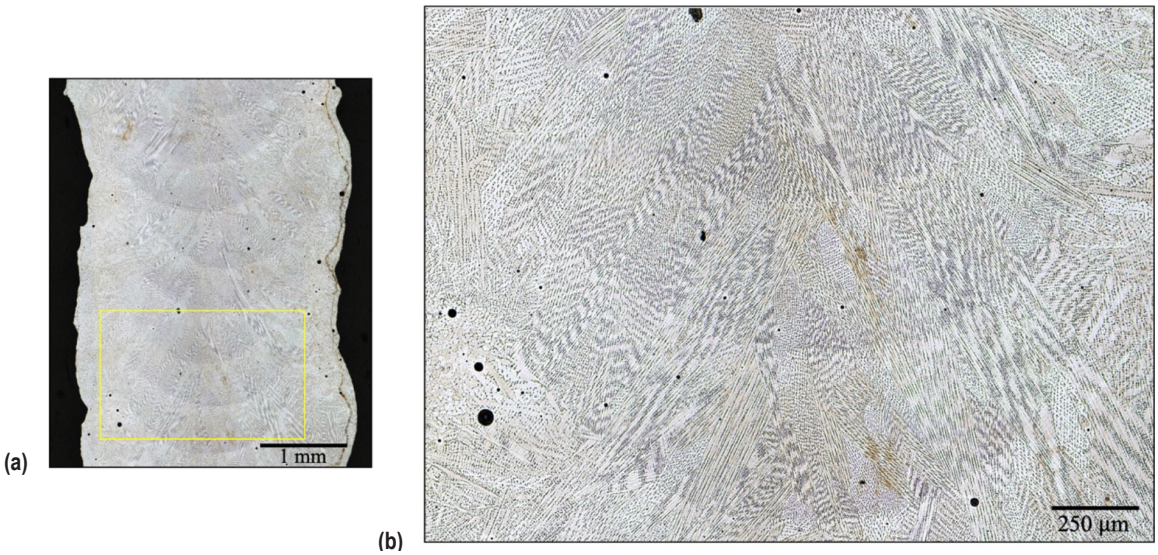

Figure 3. Optical micrographs: (a) showing the representative cross section microstructure of as-built DED NASA HR-1; (b) a closeup, more detailed image from the yellow box seen in (a). This single-pass DED panel was deposited with a thickness of approximately 3.175 mm (1070 Watts laser). The build direction is vertically upward.

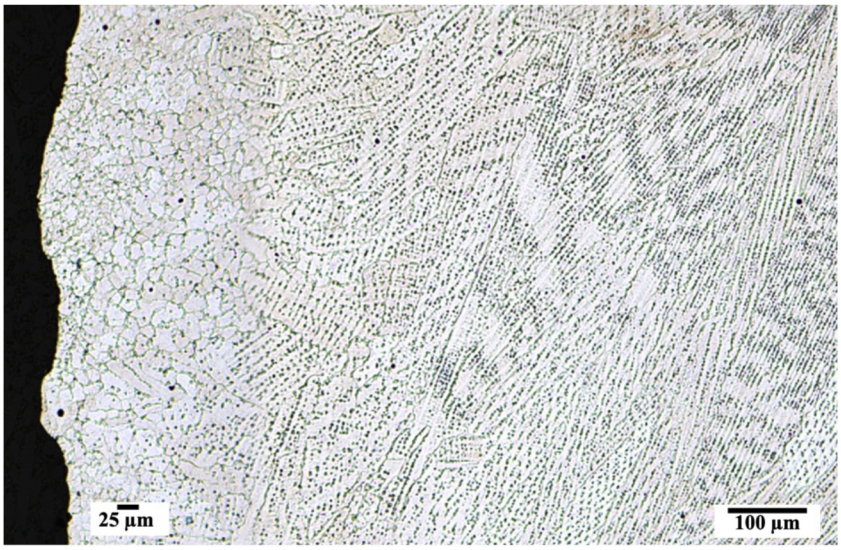

Figure 4. Closeup view of the dendritic structure in the as-built single-pass DED NASA HR-1.

The main element composition distribution across the columnar dendrites was determined by EDS. Figure 5 shows an example of titanium segregation in an as-built, 3.175-mm-thick, single-pass DED NASA HR-1 panel where the titanium distribution profile was revealed through the use of EDS line scans. A large variation in titanium concentration, the major hardening element, can be clearly seen over a 250 µm distance. The nominal 2.5 wt% titanium varies considerably between a minimum of 0.6% to a maximum of about 17%. Titanium concentration exceeds 7% in at least seven spots. A closeup view for titanium concentration up to 8% (Figure 5(b)) reveals that titanium concentration fluctuates intensely between 0.3%–5% in most areas. Similar highly fluctuating titanium concentration profile was also present in an as-built 1-mm-thick, single-pass DED NASA HR-1 panel, as shown in Figure 6.

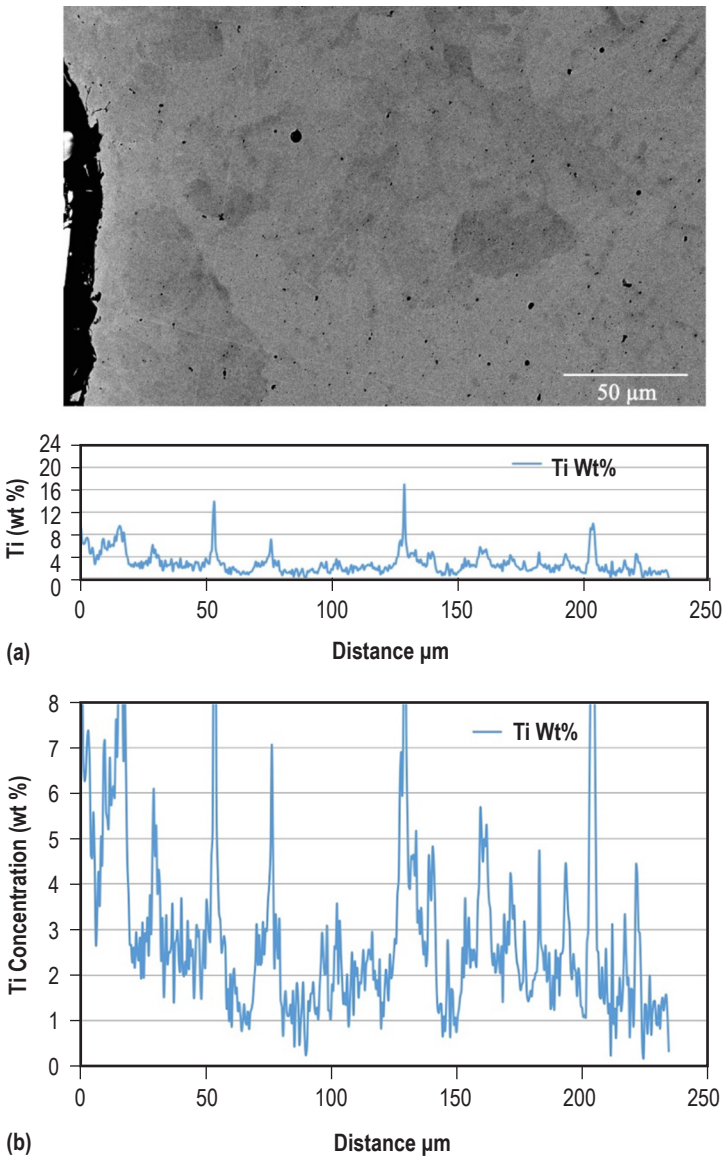

Figure 5. (a) An EDS line scan showing titanium concentration profile over a 250-µm distance in an as-built 3.175-mm-thick single-pass DED NASA HR-1 panel and (b) closeup view up to 8% reveals that titanium concentration fluctuates intensely between 0.3%–5% in most areas.

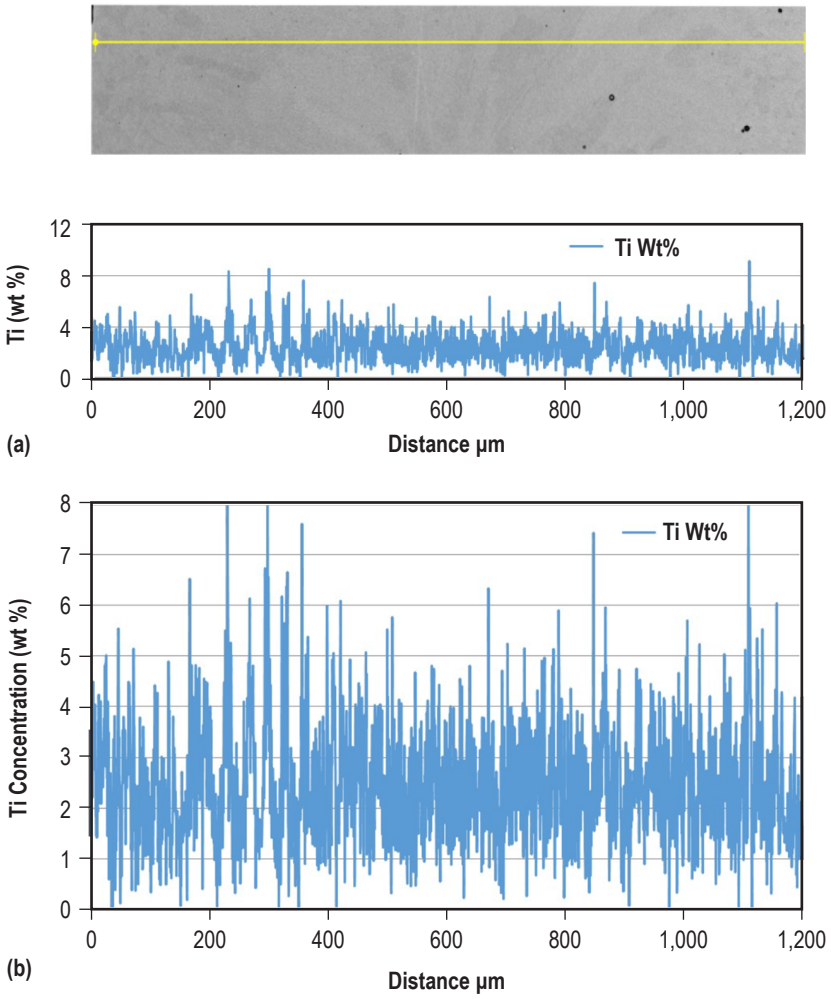

Figure 6. (a) An EDS line scan showing titanium concentration profile over a 1200-µm distance in an as-built 1-mm-thick single-pass DED NASA HR-1 panel and (b) closeup view up to 8% reveals that titanium concentration fluctuates intensely between 0.1% –5% in most areas.

3.2 Microstructure Evolution After Stress Relief and Homogenization/Hot Isostatic Pressing

Figure 7 illustrates the microstructures of single-pass DED NASA HR-1 after three different stress relief treatments. The sample that received stress relief treatment at 1700 °F exhibits dominant dendritic structure similar to that of the as-built material. The dendritic morphologies were significantly weakened with increasing the stress relief temperature. Significant microstructure changes occurred when the stress relief temperature rose to 1800 °F. The dendritic structure has almost vanished, and early stage of recrystallization has occurred after being treated at 1800 °F/1.5hr. Stress relief at 1900 °F/1.5hr led to a slightly higher degree of recrystallization, but the grain structure remains very heterogeneous (see Figure 7(c) and 7(d)). During the DED process, the rapid heating and cooling of the melt pools along with the molten metal volume change upon solidification result in the residual stress buildup in the parts. The driving force for

recrystallization is the residual stress from the AM process.[19,21] It is apparent that the residual stress for single-pass DED NASA HR-1 is quite high, and partial recrystallization occurs when the stress relief temperature is higher than 1800 °F.

Figure 7. Effects of stress relief temperature on microstructure evolution for single-pass DED NASA HR-1. The stress relief conditions are (a) as-built, (b) 1700 °F/1.5hr, (c) 1800 °F/1.5hr, and (d) 1900 °F/1.5hr.

After stress relief at 1800 °F/1.5hr, the panel samples were subjected to a homogenization cycle of 2125 °F/3hr. It is obvious that a high degree of recrystallization and grain growth had taken place after the homogenization treatment as shown in Figure 8(a). The average grain size is quite large, and many grains in the material are larger than 250 μm in diameter. The large grain structure can be attributed to the large melt pool dimensions in these single-pass DED samples. It is worth noting that the homogenized sample displays smaller grains near the surface and larger grains toward the center regions. The uneven grain size distribution can be attributed to faster melt pool cooling rate at the part periphery than in the part center during the DED process. Upon the completion of the homogenization treatment, the samples were cooled rapidly through the argon quench method, and the microstructure appears free of η-phase (Figure 8(a)). When the samples were subjected to a HIP cycle at an elevated temperature, abundant η-phase developed at grain boundaries as shown in Figure 8(b). It is worth noting that titanium segregation has migrated from the interdendritic regions in the as-built DED panels to grain boundaries after HIP due to recrystallization and grain growth. The precipitation of η-phase is very sensitive to the cooling rates. At the end of the HIP cycle, the parts have to be cooled down slowly in furnace in order to allow gradual reduction in chamber pressure and temperature. As a result, η-phase formed at grain boundaries when the material cools slowly through the η-phase forming temperature range of 1750–1350 °F.[22]

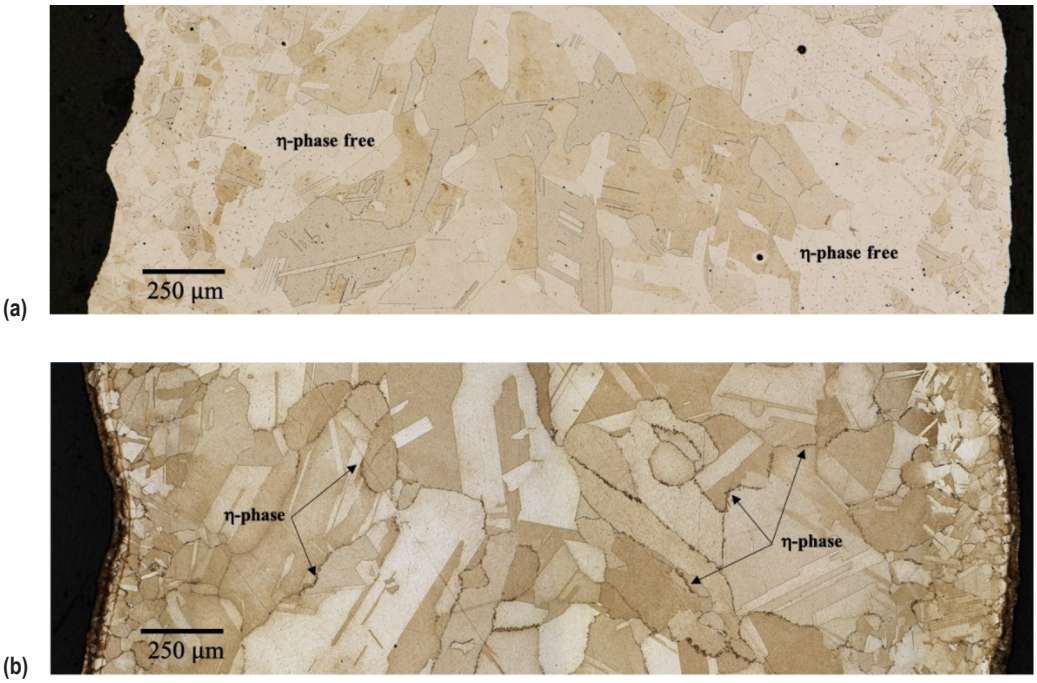

Figure 8. Macrostructure of 3.175-mm-thick single-pass DED NASA HR-1 after (a) homogenization at 2125 °F/3hr and (b) HIP at an elevated temperature.

Figure 9 shows titanium concentration profile over a 750-μm distance in a homogenized 1-mm-thick single-pass DED NASA HR-1 panel. It is apparent that titanium segregation in DED NASA HR-1 has been reduced by the homogenization treatment. A closeup view for titanium concentration up to 4% (Figure 5(b)) reveals that the fluctuation of titanium concentration has been reduced from 0.3%–8% (in the as-build condition) to 1.5%–3.5% after homogenization; but in many areas, titanium concentration is still significantly higher than the nominal 2.5 wt%. High titanium segregation at grain boundaries is not normally seen in wrought NASA HR-1. The difference in grain-boundary titanium segregation between wrought and DED NASA HR-1 can be attributed to the difference in the solidification rates between DED and conventional casting processes. Comparing to the DED process, the casting process has much slower cooling (solidification) rate that allows for prolonged cooling times for the castings, permitting the slow-to-diffuse elements (such as titanium) to disperse more homogeneously. In addition, NASA HR-1 castings usually receive homogenization treatment at elevated temperatures for 24 hr, which is significantly longer than the current homogenization treatment of only 3 hr at 2125 °F for DED NASA HR-1. Thus, the slow cooling during the casting process coupled with extended homogenization treatment for cast NASA HR-1 drastically reduces titanium segregation at grain boundary and the propensity to form the detrimental η-phase after heat treatment.

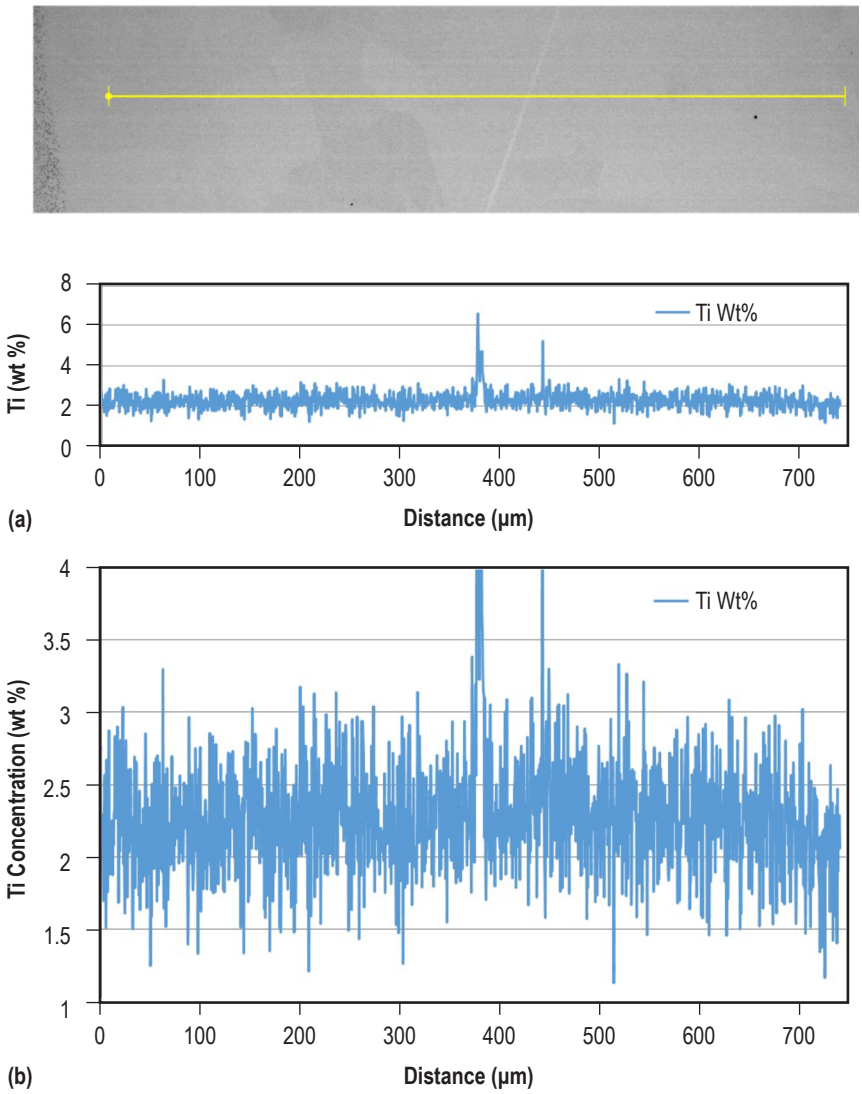

Figure 9. (a) An EDS line scan showing titanium concentration profile over a 750-μm distance in a homogenized 1-mm-thick single-pass DED NASA HR-1 panel and (b) closeup view up to 4%, which reveals that titanium concentration fluctuates moderately between 1.5%–3.5% in most areas.

3.3 Precipitation Of Grain Boundary η-Phase After Aging Treatment

After the homogenization treatment, the samples were solution annealed at 1800 °F/1hr, followed by direct water quenching. Then, the samples were aged at 1325 °F/16hr to complete the heat treatment for DED NASA HR-1. As shown in Figure 10(a), the microstructure appears η-phase-free after solution treatment as the parts were cooled rapidly from 1800 °F to ambient temperature (by forced air cooling or quenching in water) to maintain η-phase free solid solution. However, η-phase precipitated at grain boundaries after the standard aging treatment at 1325 °F/16hr as shown in Figure 10(b). It is postulated that dissolution of η-phase has taken place at 1800 °F, but titanium concentration at grain boundaries remained quite high. As a result, copious η-phase was present along the grain boundaries after aging at 1325 °F/16hr.

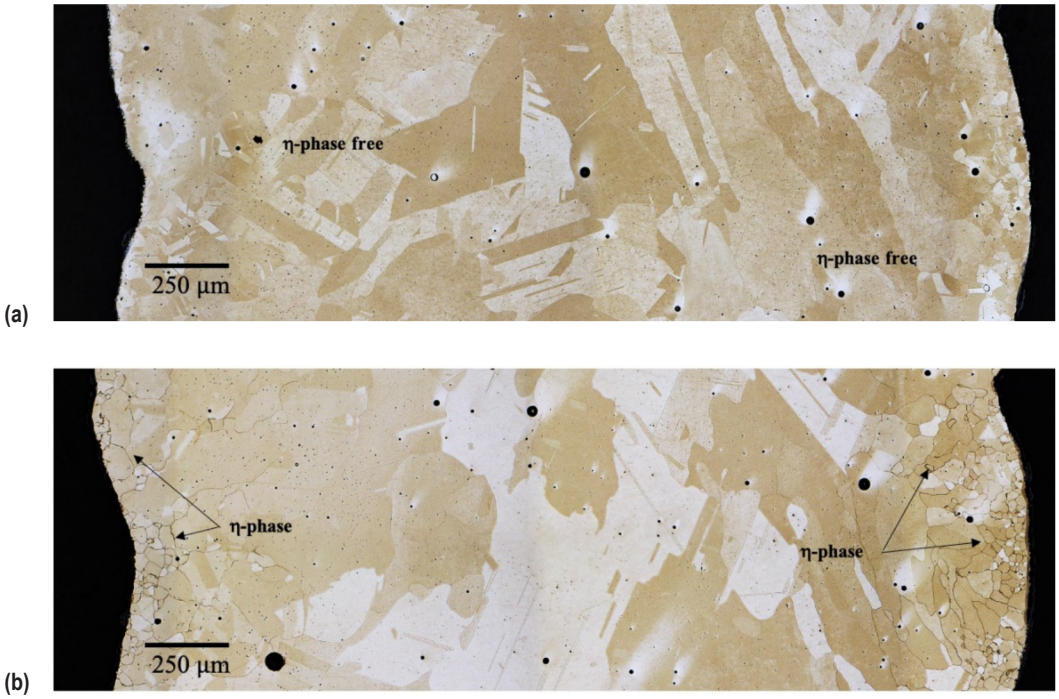

Figure 10. Macrostructure of 3.175-mm-thick single-pass DED NASA HR-1 after (a) solution treatment at 1800 °F/1hr, and (b) aging treatment at 1325 °F/16hr.

Closeup views of η-phase at grain boundaries in single-pass DED NASA HR-1 (3.175 mm) panel is given in Figure 11. The η-phase in the 3.175-mm-thick DED panel has primarily formed near the edges where the difference in grain size was observed, but it was seen to a lesser degree in the middle of panel sample after aging. However, grain-boundary η-phase is more evenly distributed through thickness in a thin single-pass (1 mm thick) DED NASA HR-1 panel after the same aging treatment at 1325 °F/16hr (see Figure 12). It is not readily known as to what causes the uneven grain-boundary η-phase distribution in the 3.175 mm single-pass DED panel. SEM examination was performed for the 3.175-mm-thick DED panel sample to see if smaller η-phase is present at grain boundaries in the middle of panel sample.

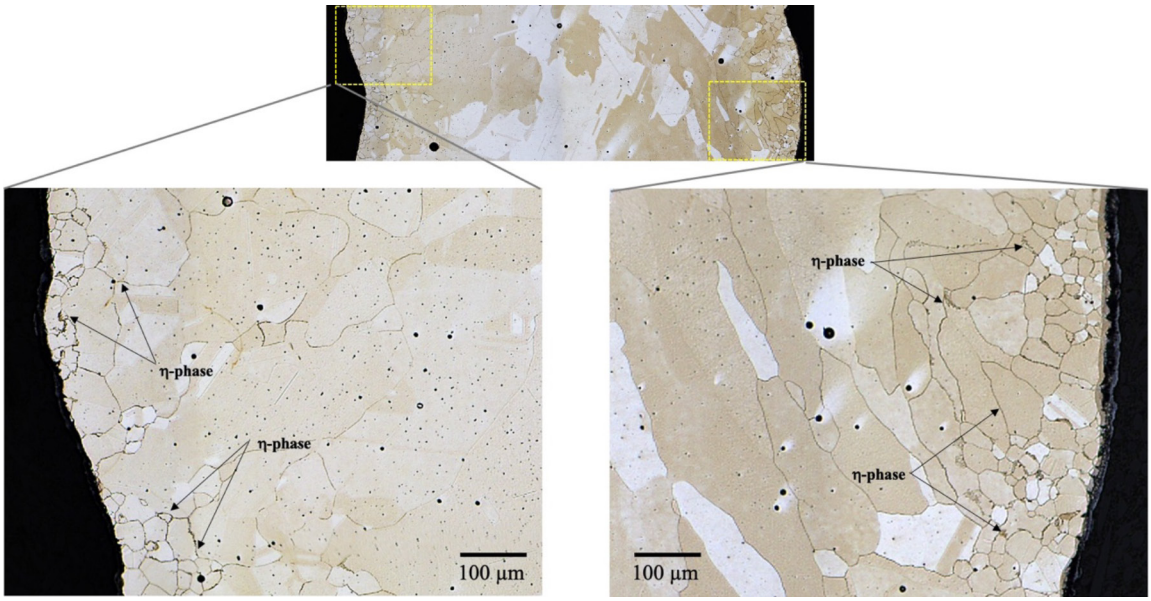

Figure 11. Closeup views of η-phase at grain boundaries in a DED NASA HR-1 single-pass panel after being aged at 1325 °F/16hr.

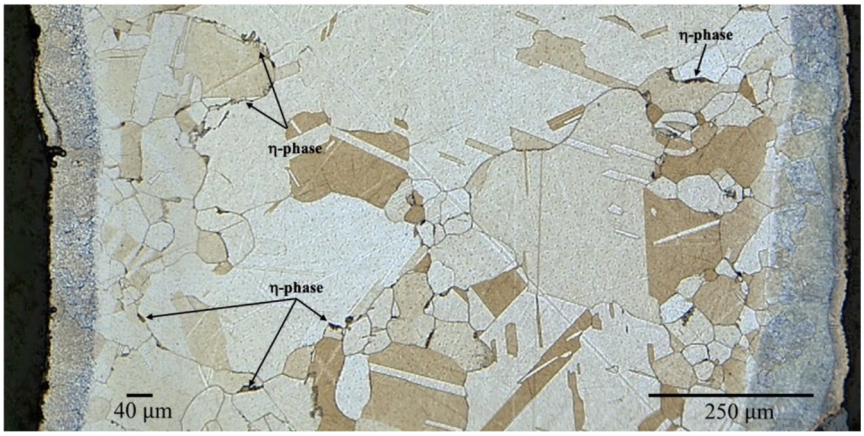

Figure 12. Grain-boundary η-phase is more evenly distributed through thickness in a thin single-pass DED NASA HR-1 panel (1 mm thick) after being aged at 1325 °F/16hr.

Grain boundary titanium concentration was analyzed using SEM-EDS to measure the degree of grain-boundary titanium segregation for the aged samples. As shown in Figure 13, titanium segregation in the aged single-pass DED NASA HR-1 is still quite high. A large variation in titanium concentration can be clearly seen over a 250 μm distance. Titanium concentration exceeds 8% in at least three spots. A closeup view for titanium concentration up to 8% (see Figure 13(b)) reveals that in most areas, the fluctuation of titanium concentration has been reduced from 0.3%–8% (in the as-build condition) to 0.6%–4% after aging. Although titanium segregation is

significantly reduced by the homogenization treatment and solution anneal, titanium concentration is still too high to prevent precipitation of η-phase at grain boundaries. There is a need to perform additional analyses to see how the homogenization process should be adjusted to mitigate titanium segregation in single-pass DED NASA HR-1.

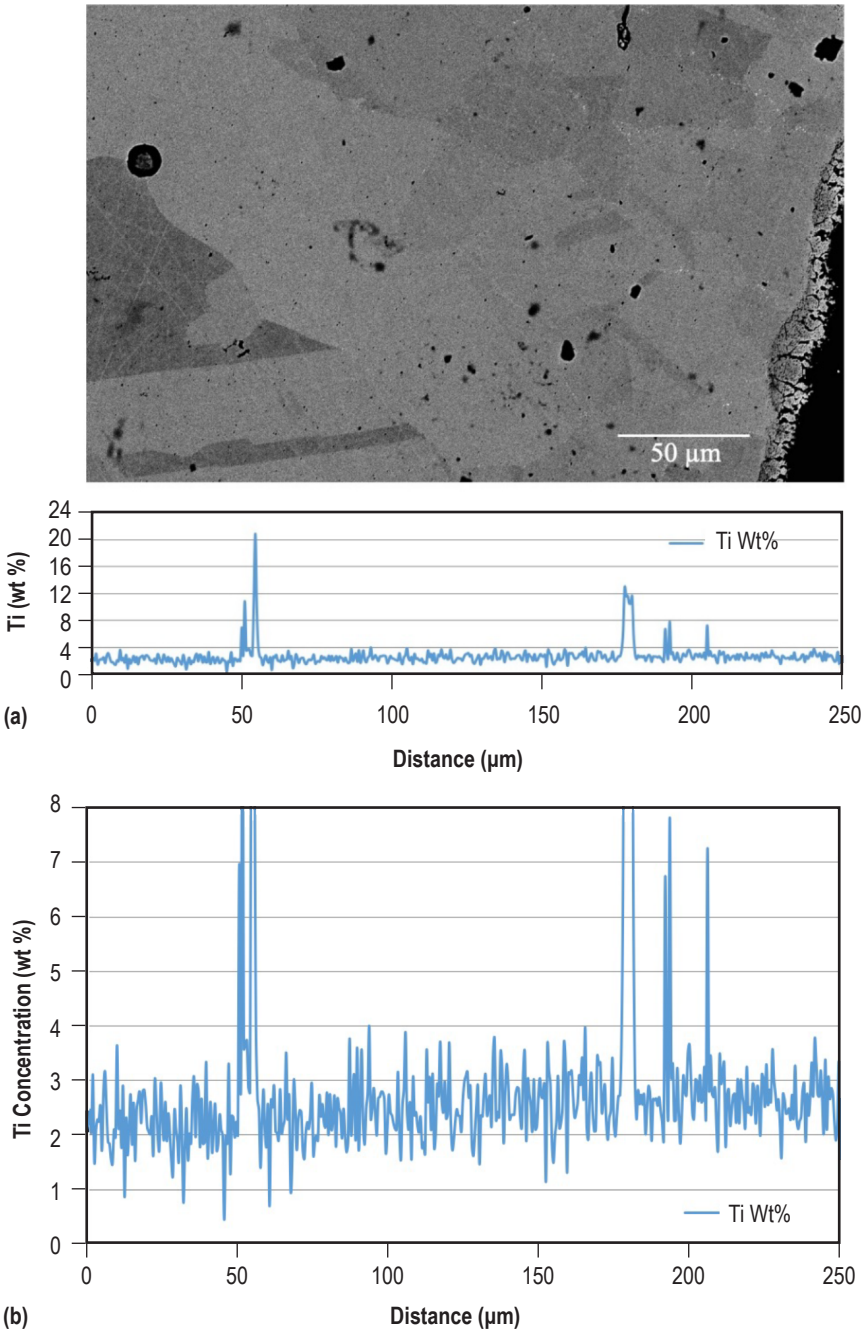

Figure 13. (a) An EDS line scan showing the typical titanium concentration profile over a 250-µm distance in aged DED NASA HR-1 and (b) closeup view for titanium concentration up to 8% reveals that titanium concentration fluctuates between 0.6% to 4% in most areas.

3.4 Mitigating Titanium Segregation Through Homogenization Kinetic Analysis

3.4.1 Determination of the Temperature Dependent Titanium Diffusivity

The presence of grain-boundary η-phase in fully heat-treated DED NASA HR-1 is a serious concern, as η-phase is brittle and has a negative impact on tensile ductility, LCF life, and HEE resistance. The segregation of titanium can be reduced by homogenization treatment at 2125 °F/3hr, but titanium concentration remains high in many localized areas. In order to further reduce titanium segregation at grain boundaries, there is a need to adjust the current homogenization treatment for DED NASA HR-1. Because of recrystallization of the as-built dendritic structure after homogenization, the degree of homogenization is connected with the grain size and titanium diffusion from grain boundaries to the grain center regions. Grain size in homogenized single-pass DED NASA HR-1 varies considerably from zone to zone, larger in the center and smaller in the periphery. As a result, the structure may have become homogeneous in the zones with finer grains, but titanium concentration may still be quite high in the boundaries of larger grains. The homogenization process will have to be conducted at higher temperatures or longer times to further reduce titanium segregation. However, the use of higher homogenization temperatures and/or longer times may lead to undesirable grain growth and serious surface oxidation. Therefore, the temperature and time of the homogenization process must be optimized to obtain an acceptable microstructure.

The homogenization process is mainly controlled by the atomic diffusion process. The solute atoms diffuse from a higher concentration at the grain boundaries to the lower concentration grain interior. The ideal homogenization process comes to an end when the solute concentration becomes uniform. However, it is difficult to determine the time required at the chosen homogenization temperature when the size of the grains varies considerably in the material. To predict the concentration of titanium atoms between the grain boundaries as a function of grain size, the diffusion coefficient (D) must be known. Diffusion coefficient is the measure of mobility of diffusing species. The diffusion coefficient in solids at different temperatures is generally found to be well predicted by the equation shown below.[23] The temperature dependence of the diffusion coefficient, D is given as:

$$D = D_o \exp\left(-\frac{Q}{RT}\right) , \tag{1}$$

where

D_o = diffusion constant (m^2/s)
Q = diffusion activation energy (J/mole)
R = gas constant (8.31 J/mole-K)
T = thermodynamic temperature (K).

Solute diffusion coefficients of titanium in nickel have been reported in a comprehensive first-principles study[24] and are shown in the blue line in Figure 14. The diffusion coefficients for titanium in JBK-75[23] were calculated using the diffusion constant (D_o) and activation energy (Q) for of titanium in γ-iron (FCC structure) and the results are also given in Figure 14 (orange line). The dotted orange lines were drawn by extrapolating from the calculated diffusion coefficients in γ-iron. Equation (1) can be rewritten as:

$$\ln D = \ln D_o - \frac{Q}{R}\left(\frac{1}{T}\right)$$

or

$$\log D = \log D_o - \frac{Q}{2.3R}\left(\frac{1}{T}\right) \ .$$

Plotting log$D$ versus 1/T yields a straight line, for which the slope is equal to –Q/2.3R, and the activation energy Q and D_o can be estimated by plotting log$D$ versus 1/T. Such plot is called an Arrhenius plot.[25]

As shown in Figure 14, the diffusion coefficients calculated directly from the first principles for titanium in nickel are in close agreement with those calculated using the measured diffusion constant and activation energy for titanium in γ-iron. At 2156 °F, the calculated titanium diffusion coefficient in γ-iron agrees very well with the experimentally measured titanium segregation for JBK-75.[23] The calculated titanium diffusion coefficients in γ-iron (for JBK-75) is given in Table 2. The diffusion data for titanium in NASA HR-1 is not available. Because the chemical composition of NASA HR-1 is close to that of JBK-75, it was decided that the calculated titanium diffusion coefficients for JBK-75 would be used for the homogenization kinetics analysis for DED NASA HR-1.

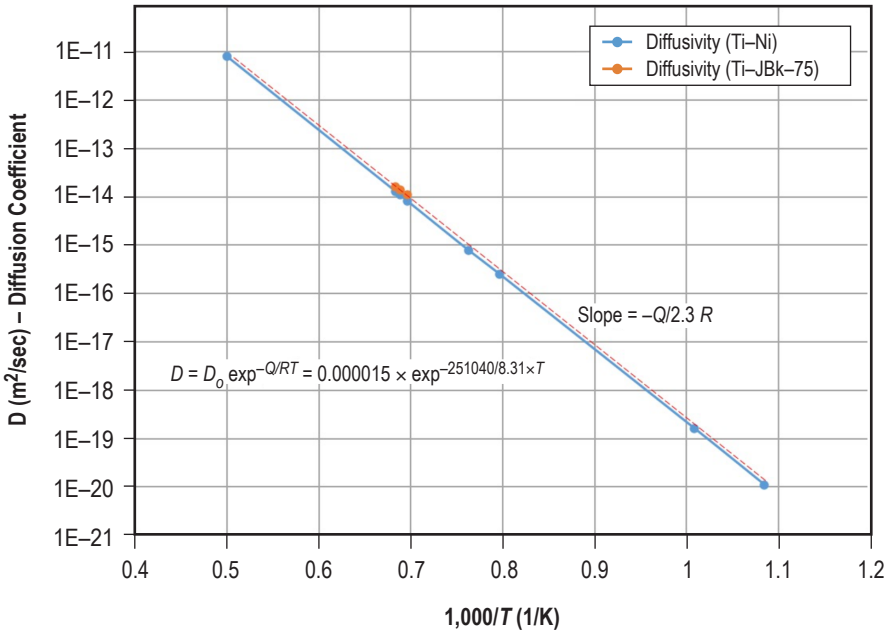

Figure 14. Diffusion coefficient (also called diffusivity) as a function of the reciprocal of temperature for titanium in nickel calculated using the first-principles (blue line)[24] and titanium in γ-iron (orange line).[23] Graph of log$D$ versus $1/T$ has a slope of $-Q/2.3R$.[25]

Table 2. Calculated diffusivity for Ti in Ni and Ti in JBK-75 (in γ-iron).

Temperature (F°)	Temperature (K)	1,000/T	Diffusivity (Ti in Ni)	Diffusivity (Ti in JBK-75)
3140	1999.87	0.500	8E–12	1.12E–11
2300	1533.20	0.652	3.5E–14	4.9E–14
2275	1491.53	0.670	1.7E–14	2.38E–14
2175	1463.76	0.683	1.2E–14	1.68E–14
2156	1453.20	0.688	1E–14	1.4E–14
2125	1435.98	0.696	7.9E–15	1.106E–14
2075	1408.20	0.710	4.9E–15	6.86E–15
2025	1380.42	0.724	2.9E–15	4.06E–15
1950	1338.76	0.747	1.3E–15	1.82E–15
1800	1255.42	0.797	2.3E–16	3.22E–16
1325	991.53	1.009	1.6E–19	2.24E–19
1200	922.09	1.084	1.10E–20	1.54E–20

3.4.2 Homogenization Kinetic Analysis

Homogenization kinetics analysis was performed to seek a more suitable homogenization treatment for single-pass DED NASA HR-1 that has very large grain size. The quantitative knowledge on the degree of Ti-segregation in the as-built and fully heat treated materials will help the

engineering team to determine how the standard homogenization treatment should be adjusted for single-pass DED NASA HR-1 material to minimize titanium segregation and η-phase precipitation at grain boundaries.

Simple assumptions can be made to establish a theoretical relationship between the temperature and the time required for reaching a specified homogeneous state. The temperature for homogenization for AM NASA HR-1 is traditionally chosen at 2125 °F. A model for titanium diffusion has been developed to project the effects of varying the homogenization parameters on titanium distribution.[23,26,27] The distribution of the titanium element is assumed to vary as sinusoidal distribution. A homogenization equation that is deduced from Fick's second law can be expressed as follows:

$$C(X,t) = C_m + C_A \left(\cos \frac{\pi x}{L}\right) \exp\left(-\frac{Dt\pi^2}{L^2}\right) , \quad (2)$$

where

$C(X,t)$ = titanium concentration
X = position (distance)
t = diffusion time
C_m = mean titanium concentration (after complete homogenization)
C_A = initial amplitude of titanium segregation
L = half wavelength of titanium concentration (horizontal distance between the highest and lowest concentration points of titanium)
D = diffusion coefficient of titanium in the matrix.

The titanium diffusion coefficient (D) in γ-iron was used to solve Equation 2. During the homogenization treatment, titanium atoms diffuse from the region of higher concentration (grain boundaries) to the region of lower concentration (grain center). Amplitude of titanium concentration variation at time t, is gradually decreased; but the grain size would not be changed. Therefore, the distribution of the titanium element across the grain boundaries and grain center varies periodically according to the variation law during the homogenization process.

Figure 15 shows the model predicted concentration distribution of titanium during the homogenization process when $C_A = 4.5\%$ and the average grain size is (a) 40 μm ($L = 20$ μm) and (b) 100 μm ($L = 50$ μm). As shown in figure 15, the amplitude of C_A of a sinusoidal initial distribution decays exponentially in time, and the rate depends on grain size. For grain size of 40 μm, the residual titanium segregation is reduced to 23% of C_A after homogenization at 2125 °F for 1.5 hr and to 8.7% of C_A after 2.5 hr. In contrast, when grain size is larger (100 μm), it needs 4 and 12 hr to reduce the residual titanium segregation to 53% and 16% of C_A, respectively. The degree of homogenization is judged by the values of residual titanium segregation. Therefore, it is evident that the standard homogenization at 2125 °F/3hr is adequate for treating DED NASA HR-1 with smaller grained structure (≤40 μm) but unsuitable for treating DED NASA HR-1 that has many large grains (≥100 μm).

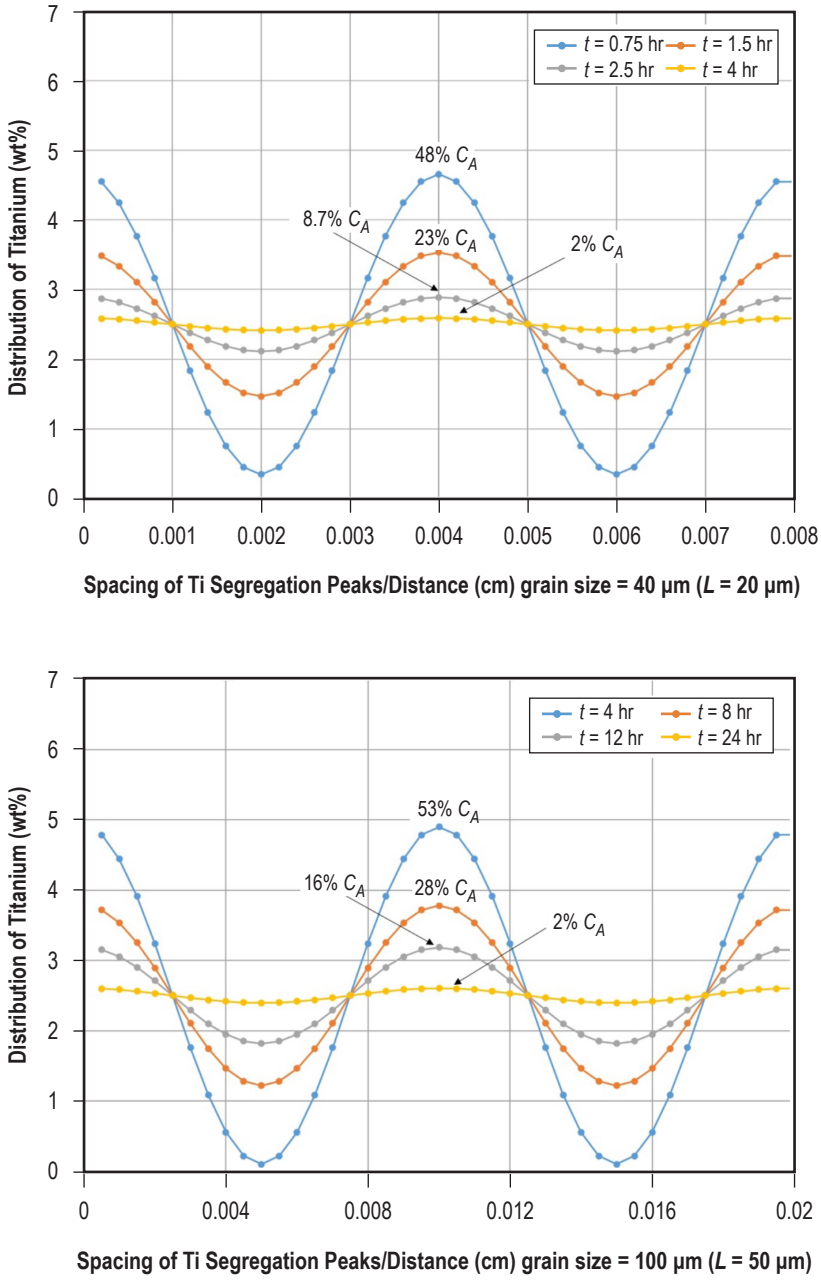

Figure 15. Titanium concentration distribution during homogenization as a function of homogenization time at 2125 °F, assuming $C_A = 4.5\%$ (Max titanium: 7%) and average grain size is (a) 40 µm ($L = 20$ µm) and (b) 100 µm ($L = 50$ µm).

The data obtained from Figure 15 indicates that the regime for homogenization should be chosen with allowance for the variation of grain size in DED NASA HR-1. For grains larger than 50 µm in diameter, higher temperature or longer duration should be considered in order to achieve homogeneous structure. However, the use of temperatures higher than 2125 °F or longer durations

at 2125 °F may lead to undesirable grain growth and increased surface oxidation. This means that the temperature and time of the homogenization process must be optimized to obtain the desirable microstructure. The degree of homogenization of an alloy can be judged by the value of residual segregation index, δ. When $x = L/2$ and $x = 3L/2$, Equation (2) can be transformed into Equation (3)[27]:

$$\delta = \left(\frac{C_{\max} - C_{\min}}{C_{0_{\max}} - C_{0_{\min}}} \right) = \exp\left(-\frac{Dt\pi^2}{L^2} \right) , \tag{3}$$

where

$C_{0_{\max}}$ = grain-boundary solute atom concentration (highest concentration) before the start of homogenization

$C_{0_{\min}}$ = grain-center solute atom concentration (lowest concentration) before the start of homogenization.

$C_{\max}$ and $C_{\min}$ are the grain-boundary and the grain-center solute atom concentration after completion of a homogenization treatment for a duration, t. The time required to reach the desired residual segregation index δ (homogeneous level) can be expressed as the following equation [27]:

$$t = -\frac{L^2 \ln \delta}{\pi^2 D_o} \exp\left(-\frac{Q}{RT} \right) . \tag{4}$$

It is significant to note that a two-fold decrease in segregation wavelength (L, half of the grain diameter) would result in a four-fold decrease in the homogenization time (t). The homogenization process for DED NASA HR-1 is mainly based on the diffusion of titanium atoms from a higher concentration location at the grain boundaries to the lower concentration grain center. Figure 16 shows the predicted homogenization kinetics (titanium diffusion) for DED NASA HR-1 for reaching the residual segregation index (δ) of 0.1 and 0.2. It can be clearly seen that homogenization time decreases with an increase of homogenization temperature for the same grain size, and small-grained material (lower L values) has a great advantage in achieving homogeneous microstructure in shorter time than that in large grained material. The current homogenization treatment for DED NASA HR-1 is 2125 °F/3hr. According to the homogenization kinetics curves at the target residual segregation index (δ) of 0.1, the combinations of temperature and time are 2125 °F/5.3hr and 2125 °F /14.8hr for grain size of 60 μm (L = 30 μm) and 100 μm (L = 50 μm), respectively. When the target residual segregation index (δ) is increased to 0.2, the homogenization times are reduced to 3.7 hr and 10.3 hr for grain size of 60 μm (L = 30 μm) and 100 μm (L = 50 μm), respectively. Based on the homogenization kinetic analysis, it is apparent that the current standard homogenization at 2125 °F/3hr is not adequate for DED NASA HR-1 panels that have many grains larger than 100 μm.

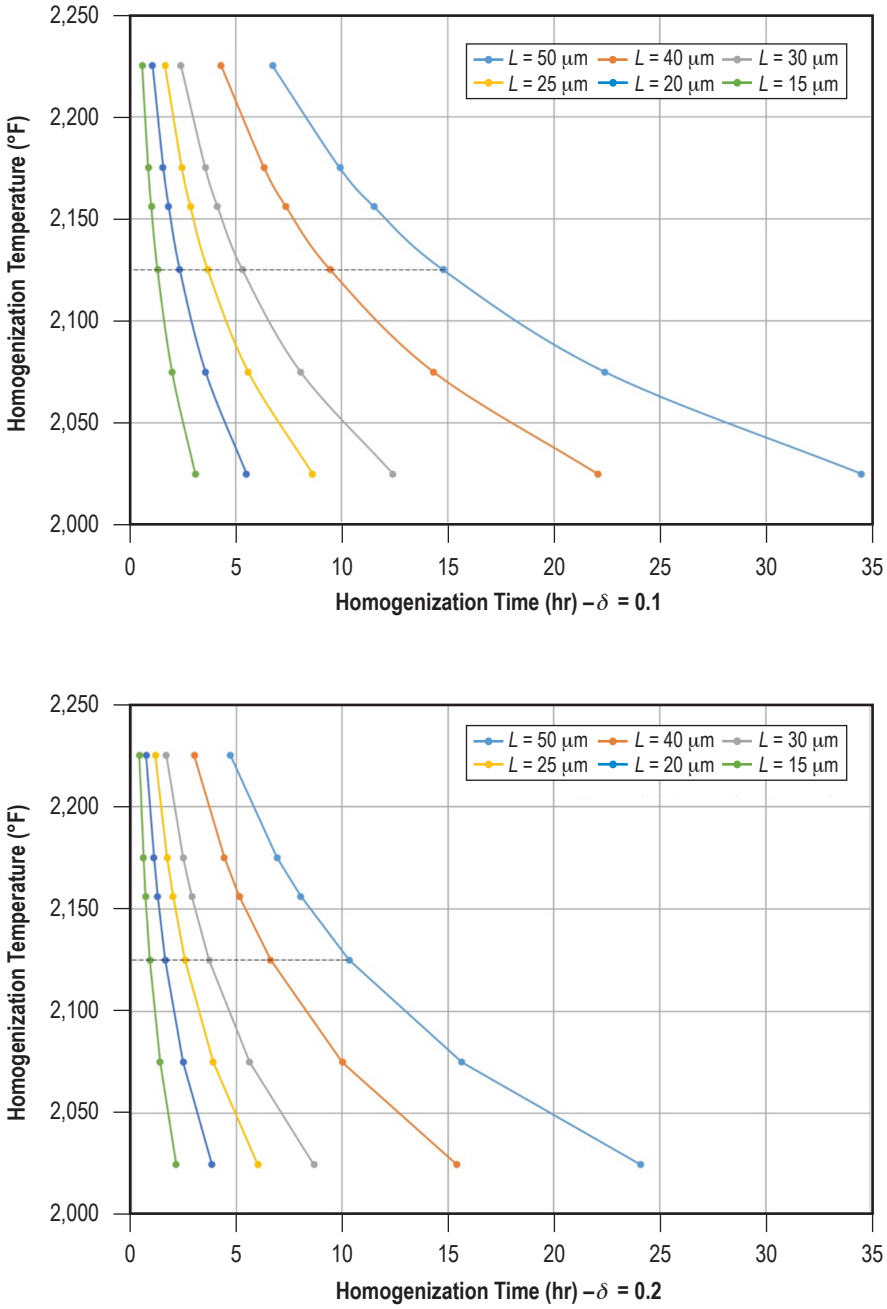

Figure 16. The predicted homogenization kinetic curves for DED NASA HR-1 for reaching the residual segregation index (δ) of (a) 0.1 and (b) 0.2. The homogenization time decreases with an increase of the homogenization temperature for the same grain size.

Titanium segregation amplitude can be slightly reduced through changes in the stress relief (SR) and solution anneal (SA) practice by increasing the temperature to 1950 °F. The effects of pre-homogenization stress relief at 1950 °F/3hr and post-homogenization solution anneal at 1950 °F/3hr are shown in Figure 17. Assuming $C_A = 4.5\%$ and average grain size is 80 μm ($L = 40$ μm), titanium

segregation amplitude can be reduced by additional 10% (from 48% to 37.6% C_A) by performing 1950 °F/3hr stress relief treatment, followed by 2125 F/3hr homogenization treatment (HOM) and 1950 °F/3hr solution anneal (3hr SR + 3hr HOM + 3hr SA) before aging treatment. When the homogenization time is extended to 6 hr at 2125 °F, titanium segregation amplitude can be reduced by an additional 5% (from 23% to 18% C_A), with the same stress relief and solution anneal before and after homogenization (3hr SR + 6hr HOM + 3hr SA). Increasing the homogenization time to more than 6 hr may be problematic, as the furnaces will be tied up longer and result in a production bottleneck, in addition to the risks of increased surface oxidation and grain growth.

Another option to decrease titanium segregation is increasing the homogenization temperature to 2175 °F or higher temperatures to shorten the homogenization time; but homogenizing at such high temperatures will increase the risks of undesirable grain growth, accelerated oxidation of the surface, and potential growth of internal pores. Therefore, homogenization at 2175 °F or higher temperatures is not recommended for DED NASA HR-1. The homogenization kinetics analysis results obtained in this study will be experimentally verified by homogenizing the DED panels at the selected homogenization time to compare the model-predicted and experimentally measured titanium concentration at grain boundaries.

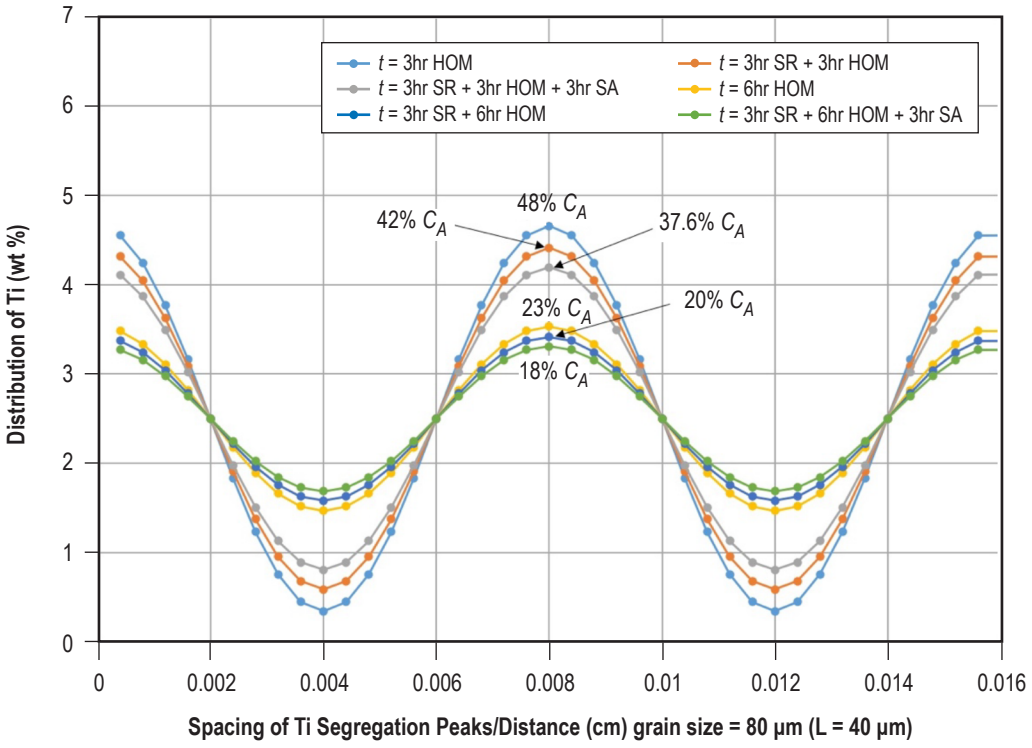

Figure 17. The effects of prehomogenization stress relief at 1950 °F/3hr (3hr SR) and post-homogenization solution anneal at 1950 °F/3hr (3hr SA), assuming $C_A = 4.5\%$ (Max titanium: 7%) and average grain size is 80 µm. Titanium segregation amplitude can be slightly reduced by increasing the stress relief and solution anneal temperature and time to 1950 °F/3hr.

3.5 Other Methods to Reduce Titanium Segregation and η-Phase Precipitation

Based on the homogenization kinetics analysis, the grain size in DED NASA HR-1 plays very important role for the choice of homogenization regime because it determines the distance passed by titanium element in the diffusion process. Therefore, reducing the grain size to shorten the homogenization time at 2125 °F remains a very effective option for DED NASA HR-1 to minimize titanium segregation at grain boundaries. The effective methods that can reduce titanium segregation and η-phase precipitation are discussed below.

3.5.1 Grain Size Reduction Through Directed Energy Deposited Parameter Optimization

The 3.175-mm- and 1-mm-thick DED panels were deposited with a single pass per layer process. The larger melt pool size results in the formation of large columnar grains that grow from the outer perimeter of the melt pool toward the center of the melt pool. The columnar grains often grow continuously through several melt pools due to epitaxial grain growth. As a result, the recrystallized grain size is quite large after homogenization at 2125 °F/3hr. Due to the slower cooling rate at the part center (than in the part periphery) during the DED process, the homogenized panel has very large grains in the center region. As a result, achieving a homogeneous structure is very difficult, and many grains are larger than 250 μm in diameter. The grain size in the multiple-pass DED NASA HR-1 is smaller, as the scan pattern between consecutive layers is not parallel, and the prior melt pool grain structure is broken up by the subsequent passes so that the grains in the new layers do not combine as easily with previous layers to form large columnar grains.[28] The microstructure of multipass DED NASA HR-1 is shown in Figure 18. It has been demonstrated that smaller grained microstructure can be obtained for SLM 718 by increasing the melt pool overlap rate to promote recrystallization.[21] The possibility of producing 3.175 mm and 1-mm-thick NASA HR-1 panels through multipass DED process with an optimized spot size and scan strategy will be evaluated in the future.

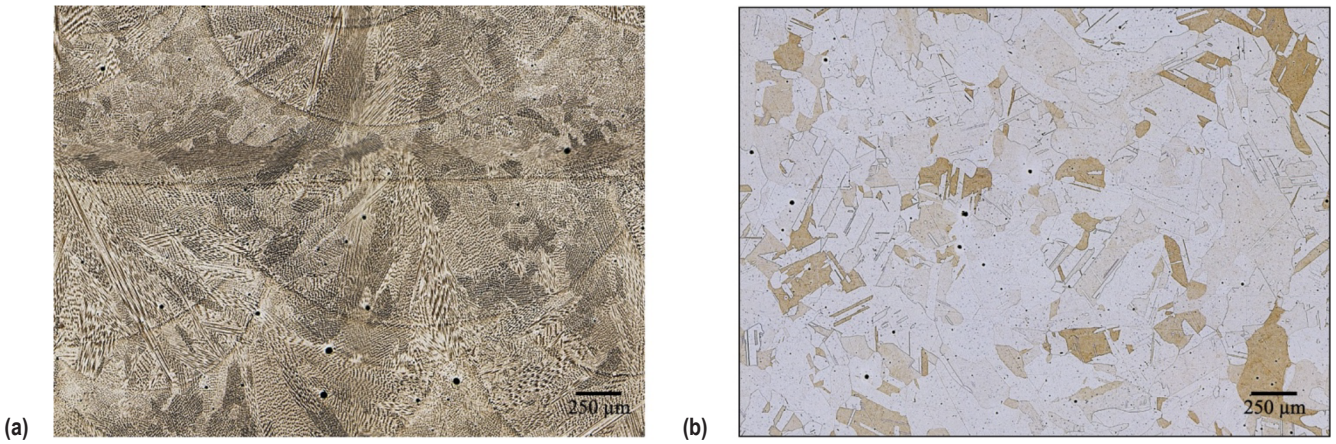

Figure 18. Multi-pass DED NASA HR-1 (a) as-built microstructure; (b) microstructure after homogenization.

3.5.2 Optimization of Chemical Composition

Additional methods that can reduce titanium segregation and mitigate η-phase precipitation at grain boundaries for DED NASA HR-1 are (1) modification of chemical composition and (2) aging treatment modification. The composition of wrought NASA HR-1 has been modified for AM using the PHACOMP method. PHACOMP was developed by Morinaga et al.[7–10,29–31] to predict austenite phase (γ) stability versus topologically closed-pack intermetallic phases (TCP) phase formation in nickel-base, cobalt-base and iron-base alloys.[30] PHACOMP method has also been applied to control the formation of geometrically closed-pack intermetallic phases (GCP), such as η-phase, for the development of high-entropy alloys.[32] TCP includes σ, χ, and Laves phases, while GCP includes η and δ phases.[33] PHACOMP uses a parameter, *Md*, which is an average *d*-electron energy above the Fermi energy level of alloying transition metals, to estimate the solid solubility of FCC (face centered cubic) γ-matrix. PHACOMP can determine a critical *Md* value, above which microstructure instability occurs.

Currently, the threshold *Md* value that must be kept below to avoid η-phase formation for NASA HR-1 is not known. Since η-phase in A-286 and JBK-75 can be kept to a very low level after heat treatment, the *Md* levels of A-286 and JBK-75 are used as the estimated critical threshold value for AM NASA HR-1.[1] Therefore, the *Md* value for DED NASA HR-1 was kept very close to that of A-286 and JBK-75 to improve the γ-matrix stability. Based on the above approaches, the chemical composition for DED NASA HR-1 has been optimized as shown in Table 3. The powder composition used for the present study is NASA HR-1 Rev 2 (revision 2). NASA HR-1 Rev 3 (revision 3) represents the latest revision that has lower *Md* value (0.913) than that in Rev 2 (0.922) as shown in Table 3. The reduction of titanium content and lower *Md* value in Rev 3 is expected to reduce titanium segregation and decrease the volume fraction of grain-boundary η-phase. Additionally, minimizing chemical variability among different powder lots will avoid the necessity of maintaining extremely tight heat treatment controls and provide the best possible DED NASA HR-1 products for LRE program applications.

Table 3. Evolution of optimal formulation for DED NASA HR-1 (wt%).

Alloy	Fe	Ni	Cr	Mo	V	W	Co	Ti	Al	Mn	Md
Wrought NASA HR-1	38.90	34.10	15.50	2.40	0.30	2.20	3.50	2.80	0.30	–	0.928
NASA HR-1 Powder Rev 2	39.80	34.00	15.50	2.20	0.32	2.10	3.30	2.50	0.25	–	0.922
NASA HR-1 Powder Rev 3	41.20	34.00	14.60	1.80	0.30	1.60	3.80	2.40	0.25	–	0.913
Wrought A-286	55.20	25.00	15.00	1.30	0.30	–	–	2.00	–	1.50	0.912
JBK-75 Powder MSFC	51.13	30.20	14.75	1.25	0.30	–	–	2.10	0.25	–	0.910

3.5.3 Aging Treatment Modification

Aging treatment for NASA HR-1 promotes precipitation of the strengthening γ' phase (Ni_3Ti).[1] It was recently discovered that the standard single-step aging practice (1325 °F/16hr for wrought NASA HR-1) was unable to prevent brittle η-phase (Ni_3Ti) precipitation for DED NASA HR-1 (Rev 2) due to high magnitude of Ti segregation at grain boundaries. Therefore, it

was decided that the aging temperature should be lowered to mitigate η-phase precipitation. But lowering the aging temperature would result in 5%–10% reduction in tensile strength. In order to offset the strength drop when the material is aged at a lower temperature, the standard single-step aging treatment was modified into a two-step aging process. Two-step aging treatment is commonly used for age-hardenable superalloys to maximize strength and to develop the best combination of short-term tensile and long-term creep properties.[34] In γ' strengthened superalloys, the first aging treatment (higher temperature) precipitates secondary γ' precipitates, and finer secondary or tertiary γ' precipitates during the second-step aging (lower temperature).[35,36]

Two-step aging treatment can vary considerably according to the alloy type and the design objectives. For DED NASA HR-1, the first aging step is carried out at a temperature slightly lower than 1325 °F to ensure adequate precipitation of γ' precipitate that is important to prevent a drastic strength reduction. The second aging step is conducted at 1200 °F or a lower temperature to offset the strength drop (arising from lower aging temperature for the first step) by precipitating finer γ' precipitate. Comparison of gain-boundary η-phase precipitation after aging at 1325 °F/24hr and 1275 °F/16hr is shown in Figure 19. The volume fraction of grain-boundary η-phase is quite high after aging at 1325 °F for 24 hr as shown in Figure 19(a). In contrast, very few isolated η-phase was present at grain boundaries after aging at 1275 °F/16hr (Figure 19(b)). The most predominant mechanism of η-phase precipitation during aging treatment is $\gamma' \rightarrow \eta$ transformation. The two-step aging treatment is specifically designed to improve the microstructure stability by retarding the $\gamma' \rightarrow \eta$ transformation during aging treatment. Thus far, two promising two-step aging treatments, 1275 °F/16hr + 1200 °F/16hr and "1275 °F/16hr + 1150 °F/16hr, have been selected for further evaluation through tensile testing."[37]

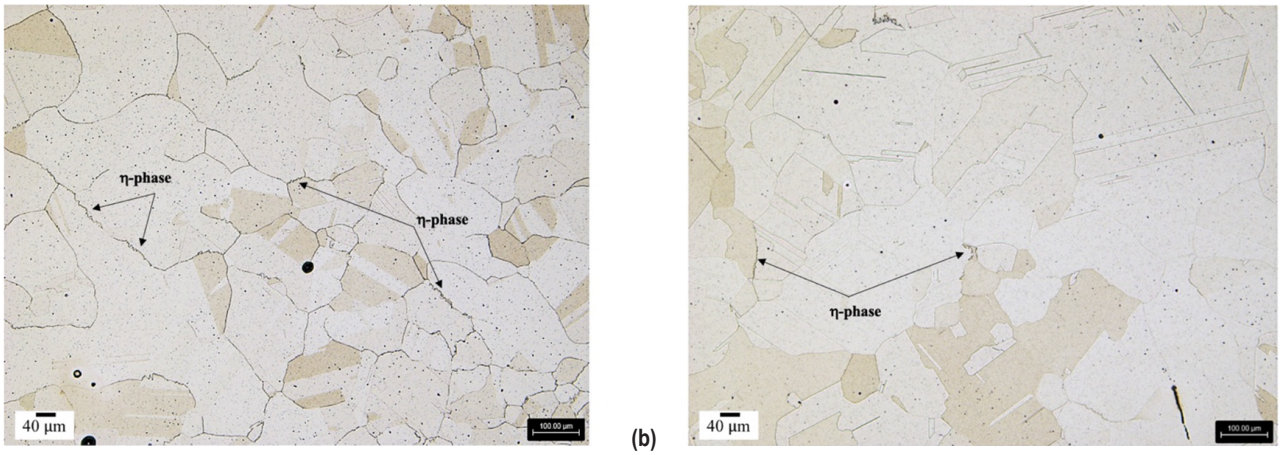

Figure 19. Grain-boundary η-phase precipitation in multi-pass DED NASA HR-1 after (a) aging at 1325 °F/24hr, (b) aging at 1275 °F/16hr.

4. SUMMARY AND CONCLUSIONS

Segregation evolution of titanium during DED process and after high-temperature homogenization in DED NASA HR-1 was thoroughly investigated. The as-built single-pass DED NASA HR-1 with wall thicknesses of 3.175 mm and 1 mm is characterized by large melt pools and epitaxial dendrite growth through several layers. SEM-EDS analysis found that there is significant titanium segregation in the as-built structure. Recrystallization and grain growth occur during homogenization treatment and titanium segregation migrates from the interdendritic regions to grain boundaries after homogenization treatment. As a result, the grain size in DED NASA HR-1 plays a very important role for the choice of homogenization regime because it determines the distance passed by titanium element in the diffusion process.

Segregation of titanium in single-pass DED NASA HR-1 is difficult to control because grain size varies considerably after recrystallization, larger in the center and smaller in the periphery. The homogenization kinetics analysis indicates the current homogenization treatment at 2125 °F/3hr is not adequate to reduce titanium segregation to an acceptable level for single-pass DED NASA HR-1. Extending the time to 6 hr at 2125 °F can achieve a higher degree of homogenization for smaller grains, but it is still unable to reduce titanium segregation to a very low level for grains that are larger than 60 μm in diameter.

To further reduce titanium segregation in the large grained regions, the homogenization process will have to be conducted at higher temperatures or longer holds, but homogenizing at temperatures above 2125 °F will increase the risks of undesirable grain growth, accelerated oxidation of the surface, and potential growth of internal pores. Therefore, homogenization at temperatures higher than 2125 °F is not recommended for single-pass DED NASA HR-1.

Reducing the grain size of DED NASA HR-1 to shorten the homogenization time at 2125 °F is a very effective option to mitigate titanium segregation. The possibility of producing 3.175-mm- and 1-mm-thick NASA HR-1 panels using multi-pass DED process will be evaluated in future publications.

Other methods that can reduce titanium segregation and η-phase precipitation at grain boundaries will also be attempted. The chemical composition of wrought NASA HR-1 has been modified for AM using the PHACOMP method. An optimal composition (Rev 3) has been formulated by decreasing the overall *Md* value to improve the γ-matrix stability. In addition, a two-step aging treatment has been successfully developed for DED NASA HR-1 to suppress η-phase precipitation. Being able to minimize the grain size variability, titanium segregation, and grain-boundary η-phase precipitation will provide the best possible DED NASA HR-1 products for LRE applications.

REFERENCES

1. Chen, P.S.; Panda B.; and Bhat, B.N.: "NASA HR-1, A New Hydrogen Resistant Fe-Ni Base Superalloy," in *Proc. of the Fifth International Conference on the Effect of Hydrogen on the Behavior of Materials*, A.W. Thompson and N.R. Moody (eds.), September 11–14, 1994, The Minerals, Metals and Materials Society, Moran, WY, pp. 1011–1020, 1996.

2. Thompson, A.W.; and Brooks, J.A.: "Hydrogen Performance of Precipitation-Strengthened Stainless Steels Based on A-286," *Metallurgical Transactions A*, Vol. 6, No. 7, pp. 1431, doi:10.1007/BF02641935, 1975.

3. Moody, N.R.; Brooks, J.A.; and Thompson, A.W.: "Development of JBK-75 for Service in High Pressure Hydrogen Environments," *The Role of Microstructure*, 1992.

4. Smugeresky, J.E.: "Effect of hydrogen on the mechanical properties of iron-base superalloys," *Metallurgical Transactions A*, Vol. 8, pp. 1283–1289, doi:10.1007/BF02643843, 1997.

5. Thompson, A.W.: "Hydrogen-induced ductility loss in commercial precipitation-strengthened stainless steel," *Metallurgical Transactions A*, Vol. 7, pp. 315–318, 1976.

6. Raynor, D.; and Silcock, J.M.: "Strengthening Mechanisms in γ' Precipitating Alloys," *Metal Science Journal*, Vol. 4, No. 1, pp. 121–130, doi:10.1179/msc.1970.4.1.121, 1970.

7. Havalda, A.: "Influence of Tungsten on the γ' to eta Phase Transformation and Carbide Reaction in Nickel Base Superalloys," *ASM transactions quarterly*, No. 62, pp. 581–589, 1969.

8. Morinaga, M.; Yukawa, N.; Ezaki, H.; and Adachi, H.: "Solid solubilities in transition-metal-based f.c.c. Alloys," *Philosophical Magazine A*, Vol. 51, No. 2, pp. 223–246, doi:10.1080/01418610.1985.12069159, August 1985.

9. Morinaga, M.; Murata, Y.; and Yukawa, H: "Recent Progress in Molecular Orbital Approach to Alloy Design," *Materials Science Forum*, pp. 37–42, doi: https://doi.org/10.4028/ www.scientific.net/msf.449-452.37, March 2004.

10. Morinaga, M; and Yukawa, H.: "Alloy design with the aid of molecular orbital method," *Bulletin of Materials Science*, Vol. 20, pp. 805-815, doi:10.1007/BF02747420, September 1997.

11. Gradl, P.R.; Protz, C.S.; and Wammen, T.: "Additive Manufacturing Development and Hot-Fire Testing Directed Energy Deposition Inconel 625 and JBK-75 Alloys," In *AIAA Propulsion and Energy Forum*, August 19–22, American Institute of Aeronautics and Astronautics, Huntsville, AL, pp. 1–20, doi:10.2514/6.2019-4362, 2019.

12. Gradl, P.R.; and Protz, C.S.: "Technology advancements for channel wall nozzle manufacturing in liquid rocket engines," *Acta Astronautica*, Vol. 174, pp. 148–158, doi:10.1016/j.actaastro.2020.04.067, September 2020.

13. Anderson, R.; Terrell, J.; Schneider, J.; et al.: "Characteristics of Bi-Metallic Interfaces Formed During Direct Energy Deposition Additive Manufacturing Processing," *Metallurgical and Materials Transactions B*, Vol. 50, No. 4, pp. 1921–1930, doi:10.1007/s11663-019-01612-1, May 2019.

14. Gradl, P.R; Greene, S.E.; Protz, C.S.; et al.: "Additive Manufacturing of Liquid Rocket Engine Combustion Devices: A Summary of Process Developments and Hot-Fire Testing Results," In J*oint Propulsion Conference*, July 9–11, 2018, American Institute of Aeronautics and Astronautics, Cincinnati, OH, pp. 1–34, doi:10.2514/6.2018-4625, July 2018.

15. Gradl, P.R.; Protz, C.S; Fikes. J.; et al: "Lightweight Thrust Chamber Assemblies using Multi-Alloy Additive Manufacturing and Composite Overwrap," In *AIAA Propulsion and Energy Forum*, August 24-28, 2020, American Institute of Aeronautics and Astronautics, Virtual Event, pp. 3787, doi:10.2514/6.2020-3787, August 2020.

16. ASTM International: "Standard for Additive Manufacturing – Post Processing Methods – Standard Specification for Thermal Post-Processing Metal Parts Made Via Powder Bed Fusion." ASTM Standards, Vol. 10.04, p. 3, doi:10.1520/F3301-18, 2018.

17. Yan, F.; Xiong, W.; and Faierson, E.J.: "Grain Structure Control of Additively Manufactured Metallic Materials," *Materials*, Vol. 10, No. 11, p. 1260, doi:10.3390/ma10111260, November 2017.

18. Neghlani, P.K.: "SLM additive manufacturing of Alloy 718 Effect of process parameters on microstructure and properties," M.S. Thesis, University West, 48 pp., doi:10.13140/RG.2.2.25434.64963, August 2016.

19. Fencheng, L.; Xin, L.; Gaolin, Y.; et al.: "Recrystallization and its influence on microstructures and mechanical properties of laser solid formed nickel base superalloy Inconel 718," *Rare Metals*, Vol. 30, No. 1, p. 433–438, doi:10.1007/s12598-011-0319-0, March 2011.

20. Zhang, F; Levine, L.E.; Allen, A.J; et al.: "Effect of heat treatment on the microstructural evolution of a nickel-based superalloy additive-manufactured by laser powder bed fusion," *Acta Materialia*, Vol. 152, pp. 200–214, June 2018.

21. Cao, J; Liu, F; Lin, X.; et al.: "Effect of overlap rate on recrystallization behaviors of Laser Solid Formed Inconel 718 superalloy," *Optics & Laser Technology*, Vol. 45, pp. 228–235, February 2013.

22. "TTP Development for DED NASA HR-1," Internal Research, NASA Marshall Space Flight Center, Huntsville, AL.

23. Mataya, M.C.; Edstrom, C.M.; Krenzer, R.W.; and Doyle, J.H.: "Segregation Effects in JBK-75," Technical Report RFP-2925, Rockwell International Corporation, Golden, CO, 40 pp., December 21, 1979.

24. Hargather, C.Z.; Shang, S.L.; and Liu, Z.-K.: "Data set for diffusion coefficients and relative creep rate ratios of 26 dilute Ni-X alloy systems from first-principles calculations," *Data in Brief*, Vol. 20, pp. 1537–1551, October 2018.

25. University of Tennessee Department of Materials Science and Engineering: "Diffusion: MSE 201 Callister Chapter 5," <https://www.coursehero.com/file/13499074/Chapter-5-Diffusion/>, 2007.

26. Purdy, G.R.; and Kirkaldy, J.S.: "Homogenization by Diffusion," *Metallurgical Transactions*, Vol. 2, pp. 371–378, February 1971.

27. Hao, Y.; Cao, G.; Li, C.; et al.: "Solidification Structures of Fe–Cr–Ni–Mo–N Super-austenitic Stainless Steel Processed by Twin-roll Strip Casting and Ingot Casting and Their Segregation Evolution Behaviors," *ISIJ International*, Vol. 58, No. 10, pp. 1801–1810, 2018.

28. Katsarelis, C.; Chen, P.S.; Gradl, P.; et al.: "Additive manufacturing of NASA HR-1 Materials for Liquid Engine Component Applications," Paper Presented at 2019 December JANNAF Meeting, Tampa, FL, December 9–13, 2019.

29. Morinaga, M.; Yukawa, N.; and Adachi, H.: "Alloying Effect on the Electronic Structure of Ni_3Al (γ)," *Journal of the Physical Society of Japan*, Vol. 53, No. 2, pp. 653–663, 1984.

30. Morinaga, M.; Yukawa, N.; Adachi, H.; and Ezaki, H.: "Superalloys," E.A. Loria (eds), *The Minerals, Metals & Materials Society*, Warrendale, PA, pp. 523–532, 1984.

31. Morinaga, M.; Yukawa, N.; and Adachi, H.: "Alloying effect on the electronic structure of BCC Fe," *Journal of Physics F: Metal Physics*, Vol. 15, No. 5, pp. 1071–1084, 1985.

32. Sheikh, S.; Klement, U.; and Guo S.: "Predicting the solid solubility limit in high-entropy alloys using the molecular orbital approach," *Journal of Applied Physics*, Vol. 118, No. 19402 doi:10.1063/1.4935620, 2015.

33. Ducki, K.J.: "Analysis of the Precipitation and Growth Processes of the Intermetallic Phases in an Fe-Ni superalloy," *Superalloys*, M. Aliofkhazraei (ed.), InTechOpen, doi: 10.5772/61159, November 2015.

34. Richard, B.F.: "Age-Hardenable Superalloys," *Advanced Materials & Processes*, Vol. 163, No. 6, pp. 37–42, June 2005.

35. Papadaki, C.; Li, W.; and Korsunsky, A.M.: "On the Dependence of γ' Precipitate Size in a Nickel-Based Superalloy on the Cooling Rate from Super-Solvus Temperature Heat Treatment," *Materials (Basel),* Vol. 11, No. 9:1528, 10 pp., doi:10.3390/ma11091528, September 2018.

36. Bassini, E.; Cattano, G.; Marchese, G.; et al.: "Study of the Effects of Aging Treatment on Astroloy Processed via Hot Isostatic Pressing," *Materials*, Vol. 12, No. 9:1517, 17 pp., doi:10.3390/ma12091517, May 2019.

37. "Two-Step Aging Treatment Development for DED NASA HR-1," Internal Research, NASA Marshall Space Flight Center, Huntsville, AL.

REPORT DOCUMENTATION PAGE

Form Approved
OMB No. 0704-0188

1. REPORT DATE *(DD-MM-YYYY)*	2. REPORT TYPE	3. DATES COVERED *(From - To)*
01–05–2021	Technical Memorandum	

4. TITLE AND SUBTITLE

Segregation Evolution and Diffusion of Titanium in Directed Energy Deposited NASA HR-1

5a. CONTRACT NUMBER
80MSFC18C0011

5b. GRANT NUMBER

5c. PROGRAM ELEMENT NUMBER

6. AUTHOR(S)

*P.S. Chen, C.C. Katsarelis, *W.M. Medders, and P.R. Gradl

5d. PROJECT NUMBER

5e. TASK NUMBER

5f. WORK UNIT NUMBER

7. PERFORMING ORGANIZATION NAME(S) AND ADDRESS(ES)
George C. Marshall Space Flight Center
Huntsville, AL 35812

8. PERFORMING ORGANIZATION REPORT NUMBER
M–1523

9. SPONSORING/MONITORING AGENCY NAME(S) AND ADDRESS(ES)
National Aeronautics and Space Administration
Washington, DC 20546–0001

10. SPONSORING/MONITOR'S ACRONYM(S)
NASA

11. SPONSORING/MONITORING REPORT NUMBER
NASA/TM–20210013649

12. DISTRIBUTION/AVAILABILITY STATEMENT
Unclassified-Unlimited
Subject Category 26
Availability: NASA STI Information Desk (757–864–9658)

13. SUPPLEMENTARY NOTES
Prepared by the Metallurgy Branch and Propulsion Systems Department, Engineering Directorate
*Jacobs ESSCA Group, NASA Marshall Space Flight Center

14. ABSTRACT
Titanium segregation in single-pass directed energy deposited (DED) NASA HR-1 is very difficult to control because grain size varies considerably and many large grains (>100 μm) are present. Therefore, homogenization kinetic analysis was performed to see how the homogenization process should be adjusted to mitigate titanium segregation. A basic model for titanium diffusion in NASA HR-1 was developed to project titanium segregation as a function of homogenization temperature, time, and grain size. The homogenization kinetic analysis provides a valuable reference on how the homogenization treatment should be adjusted to reduce titanium segregation to a very low level for DED NASA HR-1.

15. SUBJECT TERMS
liquid rocket engine, LRE, PHACOMP, phase computation, DED, directed energy deposited, AM, additive manufacturing, HEE, hydrogen environment embrittlement, NASA HR-1

16. SECURITY CLASSIFICATION OF:			17. LIMITATION OF ABSTRACT	18. NUMBER OF PAGES	19a. NAME OF RESPONSIBLE PERSON
a. REPORT	b. ABSTRACT	c. THIS PAGE			STI Help Desk at email: help@sti.nasa.gov
U	U	U	UU	48	19b. TELEPHONE NUMBER *(Include area code)* STI Help Desk at: 757–864–9658

National Aeronautics and
Space Administration
IS02
George C. Marshall Space Flight Center
Huntsville, Alabama 35812